



TECHNICAL DOCUMENT

Examination of the aircraft Examination of the left and right propellers

Accident to the Fokker - F27-500
operated by **Miniliner SRL**
registered **I-MLVT**
on 25 october 2013
at **AD Paris Charles de Gaulle (95)**

BEA

Bureau d'Enquêtes et d'Analyses
pour la sécurité de l'aviation civile

www.bea.aero



@BEA_Aero



Foreword

This document and the photographs and technical information contained herein are subject to the laws relating to communication and confidentiality embodied in European Regulation 996 of 20 October 2010.

The conclusions of this document are based on the work undertaken by the BEA (Bureau d'Enquêtes et d'Analyses pour la sécurité de l'aviation civile). They should not be used to prejudge the final conclusions of the safety investigation.

Contents

FOREWORD	2
GLOSSARY	4
1 - WORK PERFORMED	5
1.1 Examination of the site, damage to the aircraft	5
1.1.1 Examination of the site	5
1.1.2 Examination of the aircraft	5
1.1.3 Examination of the engines	9
1.1.4 Scenario of the event	10
1.2 Aircraft Information	11
1.2.1 General	11
1.2.2 I-MLVT	11
1.2.3 Dowty Propeller R193/4-30-4/61	11
1.3 Examination of the left propeller	13
1.3.1 Purpose of the examination	13
1.3.2 Equipment examined	14
1.3.3 Results	14
1.4 Examination of the right propeller	42
1.4.1 Purpose of the examination	42
1.4.2 Equipment examined	42
1.4.3 Results	42
1.5 Examination of other propellers of R193-type	46
1.5.1 Purpose of the examination	46
1.5.2 Equipment examined	46
1.5.3 Results	47
1.6 Additional Information	48
1.6.1 Previous events	48
1.6.2 Maintenance	49
2 - CONCLUSION	52
APPENDICES	54

Glossary

AAIB	Air Accidents Investigation Branch (UK)
EDS	Energy Dispersive Spectrometry
SEM	Secondary electron microscope
MSN	Manufacturer's Serial Number
OHM	Overhaul Manual
P/N	Part Number
S/N	Serial Number
TSN	Time Since New
TSO	Time Since Overhaul

1 - WORK PERFORMED

1.1 Examination of the site, damage to the aircraft

1.1.1 Examination of the site

1.1.1.1 Location of the event

The accident occurred on 25 October 2013 at around 01h20 local time on the extended runway centreline of runway 09R of AD Paris Charles-de-Gaulle (95), at an altitude of approximately 1,700 ft.

1.1.1.2 Distribution of debris

The left propeller (with the exception of blade no.2) and the forward part of the left engine were found at the end of a field in the town of Mesnil-Amelot (77) approximately 2,400 meters from the end of runway 09R, almost on the extended runway centreline (figure 1).

Blade no.2 of the left propeller was found further out approximately 1,800 meters from the end of runway 09R, aligned with the runway and the left propeller.

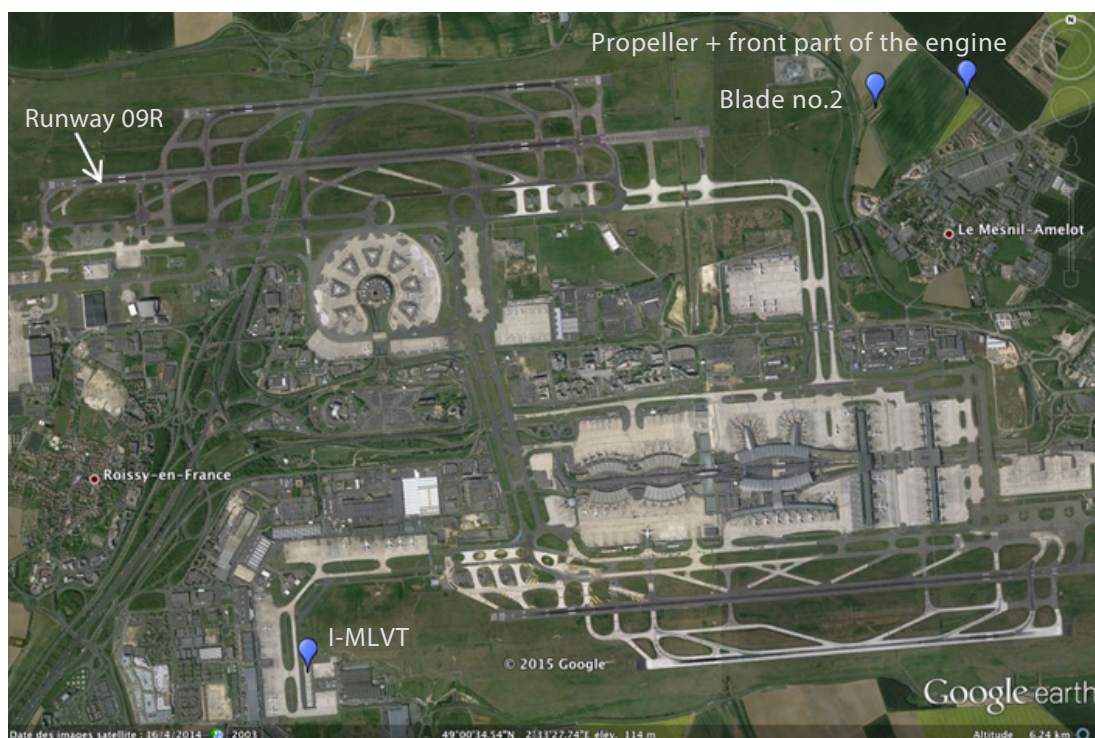


Figure 1: Distribution of debris and location of the aircraft after the event

1.1.2 Examination of the aircraft

After the accident, the aeroplane was able to return and land on 09R and park at parking area P71 of the airport. During the examination of the aircraft, it was kept on the same parking area (figure 1 and figure 2). The visual inspection of the outside of the aircraft reported damage to:

- the propeller and the left engine; the propeller was missing as was the front of the engine. Part of the left side of the engine cowling was folded backwards (figure 3);

- ❑ the left side of the fuselage at the level of the propeller, where an opening of approximately 1.20 m in height was observed, from the outside inwards (figure 3). Other smaller traces of impacts were also identified (see red arrows);
- ❑ the right side of the fuselage, where an opening of approximately 1 m in height was observed, from the inside outwards (figure 4);
- ❑ the right propeller, one of whose blades had an impact on the leading edge, at the end of the blade (figure 5).



Figure 2: General condition of the aircraft



Figure 3: Propeller missing left side - left engine damaged - opening in the fuselage and traces of impacts

The visual examination of the interior of the aircraft fuselage confirmed the direction of the deformations previously observed: from the outside inwards for the opening in the left side of the fuselage, from the inside outwards on the right side.

Wiring harnesses located between the metal fuselage and the composite inner skin were found severed at the level of the openings on the left and right sides (figure 6 and figure 7, red arrows).

A piece of blade 100 mm x 70 mm was found inserted in the fuselage, on the left side.



Figure 4: Opening in the fuselage, right propeller side



Figure 5: Impact on the leading edge of a blade of the right propeller



Figure 6: Opening left side seen from the inside, wiring harnesses cut

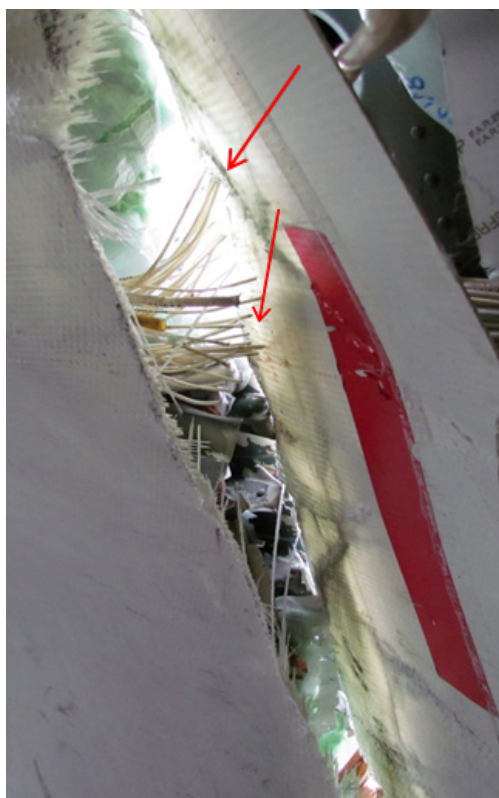


Figure 7: Opening right side seen from the inside, wiring harnesses cut

The container that was in line with the two openings at the time of the event also had perforations, the contours of which were deformed from the outside inwards on the left side, and from the inside outwards on the right side (figure 8).



Figure 8: Mail container damaged during the event

On the afternoon of 25 October 2013, a few hours after the accident, the main parts that had separated from the aircraft were located in a field at Mesnil-Amelot, a town near Paris Charles-de-Gaulle AD (Figure 1, Figure 9). They were immediately taken away.



Figure 9: left propeller with blades 1, 3 and 4 and the front part of the engine

Blade no.2 was found alone. It was broken off at the level of its preload bolt. The fracture surface showed signs of fatigue, visible to the naked eye (see § 1.3.3.5).

The rest of the left propeller with blades 1, 3 and 4, secured to the front of the engine and missing from the aeroplane, was also found in a field, cone towards the ground. Blade no.1 was only attached to the propeller by a de-icing system wire. Its end was broken, and part of the blade was missing (figure 10).



Figure 10: left propeller during lifting. Blade no.1 is only attached to the propeller by a de-icing system wire

1.1.3 Examination of the engines

The Fokker 27 registered I-MLVT was equipped with two Rolls-Royce Dart 532-7 engines. Rolls-Royce representatives visited the airport on 28 October 2013 in order to carry out an examination of the left engine (#1).

The examination revealed that:

- ❑ The engine no.1, S/N 15101, was still attached to the aircraft but the front end of the engine had separated at the location immediately forward of the 1st stage compressor casing, (figure 11).
- ❑ The reduction gear drive shaft splined drive had sheared during separation of the reduction gearbox and air intake casing.
- ❑ The vanes of the first-stage centrifugal compressor showed significant damage. Traces of friction were noted on the vanes, consecutive to contact with the compressor inlet casing, and with the air intake.
- ❑ In different places on the cooling system of the engine there were black deposits, paint blisters and burns characteristic of the presence of fire.
- ❑ The engine spool was rotated using hand pressure on the 1st stage centrifugal compressor, thus indicating that the engine had not seized.

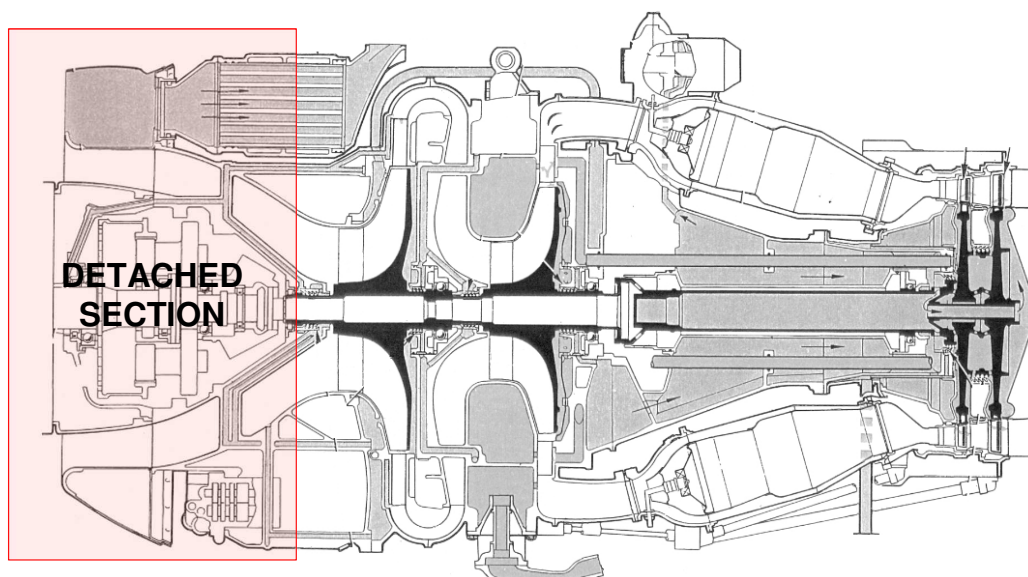


Figure 11: Sectional view of an RR Dart 532-7 engine.
In red, the separated part of engine no.1.

During the examination of the front part of the engine found in the field, it was observed that:

- ❑ traces of friction were visible on the compressor inlet casing of the first-stage compressor, consistent with the observations made on the part of the engine under the wing (friction marks on the vanes of the first-stage compressor);
- ❑ the starter was found undamaged near the front of the engine, detached, probably during the ground impact sequence;
- ❑ the flange at the rear of the air inlet, which bolts to the compressor inlet casing, had fractured around the full circumference of the flange;
- ❑ sprayed oil was visible on the rear of compressor inlet casing indicating the compressor was rotating at the time of the rupture of the front part;
- ❑ the oil cooler, torque meter pressure transmitter and two fuel transfer pipes were missing and have not been found.

No damage prior to the separation of the front part of the engine was brought to light.

The right engine was not damaged during the event and therefore was not subjected to an examination.

Finally, the spectral analysis of the CVR audio data showed that the speed of the engines was nominal from take-off to the event.

1.1.4 Scenario of the event

Examinations of the site, wreckage and engines made it possible to identify the first elements of a scenario, as follows:

- ❑ shortly after take-off, blade no.2 of the left propeller separated from the propeller due to the rupture of its preload bolt. The blade then passed through the fuselage from one side to the other and through the mail container in its path, and fell into a field;

- ❑ almost instantly, because of the imbalance caused by the loss of blade no.2, engine no.1 broke at the fracture section downstream from the 1st compressor stage, as shown in Figure 11. The detached front of the engine, while still integral with the propeller, fell into a field;
- ❑ the loss of the front part of the engine caused a fuel and/or oil leak, which ignited on contact with the hot parts of the engine. Because of the extent of damage, the fire extinguishers were inoperative, and the fire finally extinguished itself, probably due to lack of fuel;
- ❑ the crew declared an emergency and landed without further difficulty.

1.2 Aircraft Information

1.2.1 General

The Fokker F27 is a short-haul turboprop aeroplane, designed in the 1950s by the Dutch manufacturer Fokker. Its first flight was in 1955.

The fuselage of the F27-500 version is 1.5 m longer, is equipped with two Rolls-Royce Dart engines and can carry up to 52 passengers. The first flight of a F27-500 took place in 1967.

The production of the F27 was stopped in 1987. At that date, 586 aircraft (all versions) had been manufactured.

Fokker estimated that just over 70 aircraft were still in service on the date of the event. Today, these aeroplanes are mainly used for freight transport.

1.2.2 I-MLVT

- **Model:** Fokker F27-500
- **MSN:** 10373
- **Year of manufacture:** 1968
- **Operator:** Miniliner
- **Business:** Freight
- **Number of flight hours (FH):** 27791
- **Number of flight cycles (FC):** 32194
- **Engines:** Rolls-Royce Dart 532-7
- **Engine #1 S/N:** 15101
- **Engine #2 S/N:** 330
- **Propellers:** Dowty Propellers R193/4-30-4/61
- **Left propeller S/N:** DRG142/64
- **Flight hours of left propeller:** 15057
- **Right propeller S/N:** DRG106/69
- **Flight hours of right propeller:** 10813

1.2.3 Dowty Propeller R193/4-30-4/61

Propeller R193/4-30-4/61 (figure 12) is a variable pitch, 4 metal-blade propeller developed in the 1950s by Dowty Rotol Ltd.

Dowty Rotol Ltd. became Dowty Aerospace Gloucester in 1990 before becoming Dowty Propellers, a brand of GE Aviation.

Dowty Propellers estimated that approximately 150 propellers of this type were still in service as of the date of the event.

According to the OHM for the propeller, it consists of 4 main assemblies:

- ❑ the hub (figure 13), the central part of the propeller;
- ❑ the hub attachment group, enabling the assembly of the propeller to the engine shaft;
- ❑ the oil tubes used for the lubrication and operation of the pitch change mechanism;
- ❑ the blade group (figure 14) and the de-icing overshoe.

Each blade consists of a profile and a root, the latter consisting of a bearing and a preload bolt. The bearing enables the rotation of the blade in the hub, and thus the change in pitch. The bolt enables the assembly and pre-loading of the bearing. The tightening of the bolt is specified by the manufacturer. It requires the use of a hydraulic bench when mounting and dismantling the blade bearing.

The blades are assembled or disassembled with the hub by screwing or unscrewing between the central ring of the blade root bearing, which is threaded, and the arm of the hub, which is tapped. The assembly or disassembly of the blade in the hub also requires the use of a hydraulic bench, given the tightening torque values specified by the manufacturer for assembly.

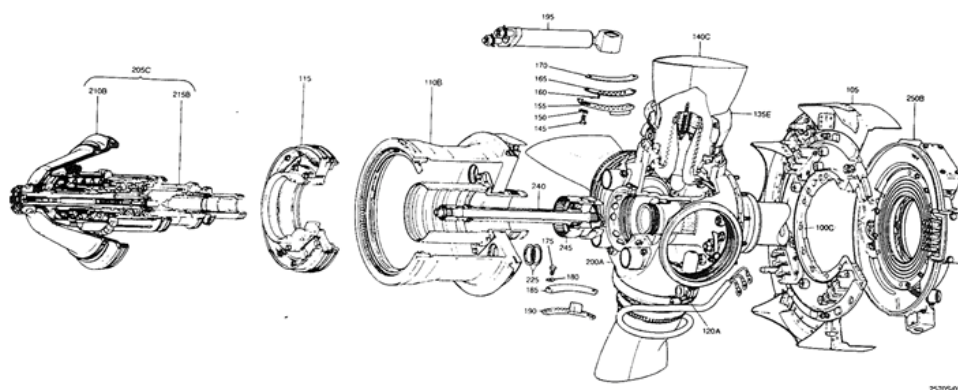


Figure 12: exploded view of propeller R193/4-60-4/61 (excerpt from the propeller OHM)

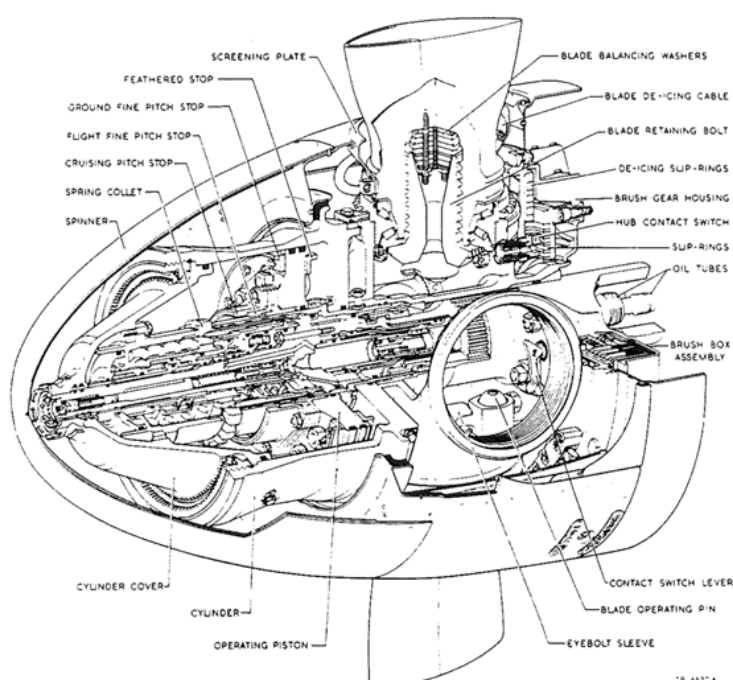


Figure 13: Drawing of the propeller hub (excerpt from the propeller OHM)

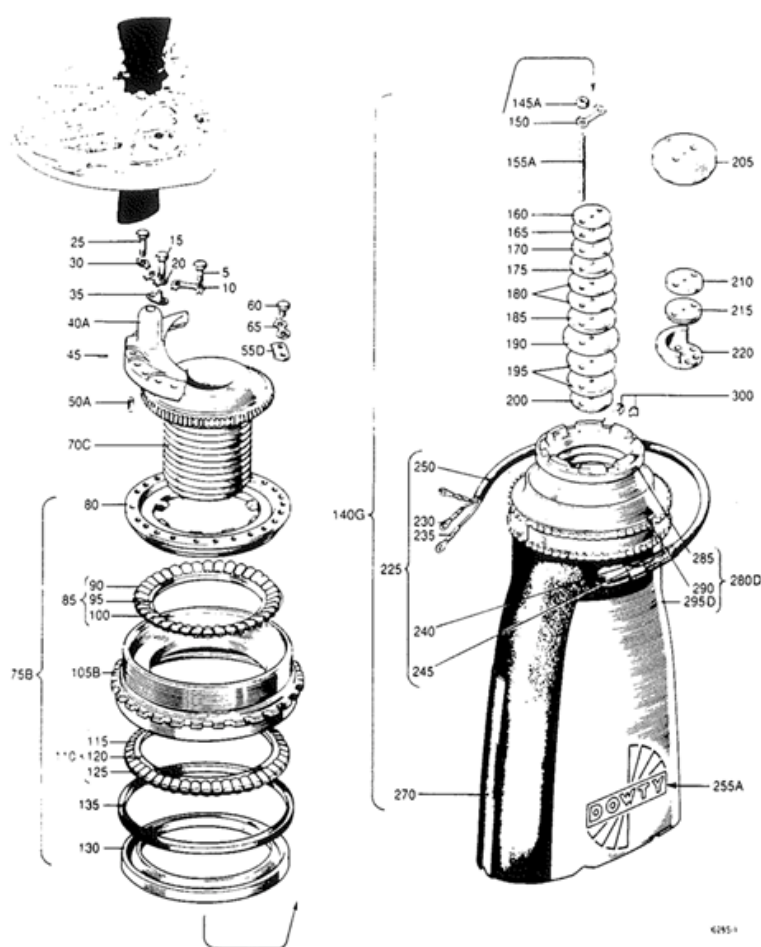


Figure 14: Exploded view of a propeller blade root, from the propeller OHM

1.3 Examination of the left propeller

1.3.1 Purpose of the examination

An initial objective of the examination of the left propeller was to characterize the general state of the propeller before the event and to determine the level of damage to the preload bolts of blades 1, 3 and 4.

Furthermore, blade no.2 separated from the left propeller due to the fracture of its preload bolt and passed through the fuselage of the aircraft. The fracture showed characteristics of crack propagation in fatigue. A detailed examination of blade no.2 and its preload bolt was carried out in an attempt to determine the origin of the fracture. The matching part, still present in the hub, was also collected and then examined at DGA-EP. The information obtained from the examinations of the two fragments of the bolt is presented in this chapter.

Finally, blade no.1 was found detached from the left propeller. Only the de-icing wire still linked the blade to the hub of the propeller. A detailed review of this blade was carried out to determine the origin of its separation from the hub.

1.3.2 Equipment examined

<p>Left propeller (seal EPAVE-2) Dowty-Propellers P/N : R193/4-30-4/61 S/N : DRG142/64</p>	<p>Blade no.1 (seal EPAVE 2-1) Dowty-Propellers P/N : RA25907-1 S/N : A139636</p>	<p>Blade no.2 (seal EPAVE 1) Dowty-Propellers P/N : RA25907-1 S/N : A140831</p>
		

<p>Part of preload bolt no.2 (taken from seal EPAVE 1) Dowty-Propellers P/N : RA58592-1 S/N : EPK 164</p>	<p>Part of preload bolt no.2 (taken from seal EPAVE 2) Dowty-Propellers P/N : RA58592-1 S/N : EPK 164</p>
	

1.3.3 Results

1.3.3.1 Disassembly of left propeller and blades 1, 3 and 4

Note: All external damage observed on the propeller before disassembly was consecutive to the loss of blade no.2 and the ensuing events, in particular the loss of the propeller and the front of the engine and their impact with the ground.

Only a few maintenance facilities in the world still carry out overhauls of Dowty Propellers R193-type propellers. None of these workshops is located in France. Since dismantling required specific hydraulic tools, it was decided to disassemble the left propeller at Proptech, in England, with the participation of representatives from the AAIB and Dowty Propellers.

Disassembly took place on 17 and 18 December 2013.

In addition to the disassembly, the following work was carried out:

- measurement of the pitch-change torque of blades 3 and 4 still in place in the hub;
- measurement of the untightening torque of blades 3 and 4 (reminder: blade no.1 was found already separated);
- measurement of the torque of the blade bearings for blades 1, 3 and 4 and the dimensions of the bearings after removal;
- magnetic particle inspection of the 3 preload bolts once disassembled.

The pitch-change torque of blades 3 and 4 still in place in the hub was measured on a hydraulic bench in accordance with the instructions in the OHM. The results are shown in Table 1.

Blades 3 and 4 were then unscrewed from the hub, and then screwed back so that the torquing index marks were realigned.

The torques required for the untightening and for realigning the index marks in their original position were then identified (Table 2).

Blade no.	Pitch-change torque	Comment
3	120-140 lb.ft	Jerky rotation
4	90-100 lb.ft	Jerky rotation
<i>OHM specifications on assembly*</i>	<i>90-190 lb.ft</i>	<i>Smooth rotation</i>

**For information purposes only, given the level of damage to the propeller*

Table 1: measurements of the pitch-change torque

Blade no.	Untightening torque	Torque on realignment
3	720 lb/psi	660 lb/psi
4	720 lb/psi	620 lb/psi
<i>OHM specifications on assembly*</i>	<i>765-786 lb/psi</i>	

**For information purposes only, given the level of damage to the propeller*

Table 2: torque measurements when unscrewing the blades from the hub

After each blade was separated from the hub, the diameter of their bearing was logged (two measurements per bearing, along two orthogonal diameters). The torque required to rotate the blade in the bearing was then measured. The bearings were then removed. The next day, the diameters of the bearings alone were once again measured to estimate the amplitude of their shrinkage after disassembly. The results are shown in Table 3. The values in red are outside the OHM specifications.

Blade no.	Bearing diameter before removal	Bearing diameter after removal	Difference (shrinkage when negative)	Bearing torque
1	6.4850" ⁽¹⁾ 6.4800"	6.4830" 6.4810"	-0.0020" +0.0010"	120 lb.ft
3	6.4820" 6.4830"	6.4800" 6.4810"	-0.0020" -0.0010"	140 lb.ft
4	6.4830" 6.4830"	6.4800" 6.4800"	-0.0030" -0.0030"	60 lb.ft
<i>OHM specifications on assembly*</i>	<6.5050"		0.0040" – 0.0045"	90-190 lb.ft

⁽¹⁾The " sign means «inch» (imperial unit). 1" is equal to 25.4 mm.

**For information purposes only, given the level of damage to the propeller.*

Table 3: measurements of bearing torque and bearing shrinkage after removal

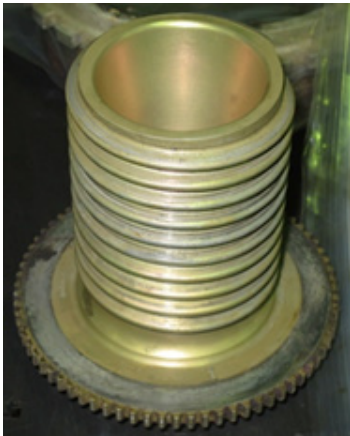
The OHM requires, when mounting the propeller, that the expansion value of the blade bearing be within a certain range. The expansion of the bearing is an indicator of the pre-loading of the preload bolt and of the bearing itself. Thus, an expansion of the bearing in the recommended range indicates optimal preloading of the bolt and the bearing.

Based on the measurements made and the values specified in the OHM, it seems that pre-loading of the preload bolt is below the nominal value. However, it is not possible to say whether the pre-loading was below the specification when the propeller was installed, if it fell below the specification between the mounting of the propeller and the accident, or was due to the event. Nor is it not possible to say whether, during the service life of the propeller, the pre-loading of the bolt changed.

The preloading value of the bearing of blade no.2 with the broken preload bolt is not known.

1.3.3.2 Magnetic particle examination of the preload bolts

Equipment examined

<p>Preload bolt no.1 taken from seal EPAVE-2 Dowty-Propellers P/N: RA58592-1 S/N: EPK 154</p>	<p>Preload bolt no.3 taken from seal EPAVE-2 Dowty-Propellers P/N: RA58592-1 S/N: EPK 155</p>	<p>Preload bolt no.4 taken from seal EPAVE-2 Dowty-Propellers P/N: RA58592-1 S/N: EPK 165</p>
		

After removal, the bolts of blades nos.1, 3 and 4 were degreased and then visually examined. The examination revealed areas of discolouration on the bolts of blades nos.3 and 4, mainly located near the bolt head, in the fillet radius or area of the first thread (figure 15). The discolourations were shown at various maintenance operators carrying out R193 propeller type maintenance. They were described sometimes as normal, and sometimes as unusual by these operators. Bolt nos.1 and 2 showed no such discolouration. After metallographic inspections carried out in these areas, it appeared that the cadmium plating was still present. Note that the cadmium plating acts as corrosion protection. This means it was the passivation layer⁽²⁾ which had been altered.

Magnetic particle inspection was then performed on the bolts, as described in the Dowty-Propellers document NDT26/M-SPM. The results are reported in **APPENDIX 1**.

On bolt nos.1, 3 and 4, surface defects were observed by magnetic particle inspection. In most cases, the defects indicated through-cavities. More rarely, the indications revealed machining striations (figure 16).

No cracks were highlighted by these means on these bolts.

Röder Präzision (a maintenance workshop located in Egelsbach in Germany that carried out the last overhaul of the propeller) indicated that their procedures for magnetic particle inspections of cadmium-plated parts require systematic de-plating of the parts before the inspection. This overcomes indications which may be related to the presence of cadmium, and not to the presence of defects. It is not possible to say whether the defects observed on bolt nos.1, 3 and 4 without de-plating would also have been highlighted after de-plating.

⁽²⁾Passive film applied to the surface of the material at the end of the plating process which significantly slows the rate of oxidation, the thickness of which is typically a few hundred nanometres

When questioned about this, Dowty Propellers replied that there was no need to strip the cadmium plating from the part before magnetic particle inspection. Cadmium stripping is not specified in the OHM or in the Dowty-Propellers document NDT26/M-SPM.

Röder Präzision also indicated that they had never detected surface defects (using a liquid indicator to reveal the potential presence of a defect) when using magnetic particle inspection on this type of preload bolt. They stated that if the slightest surface defect had been detected, given the criticality of the part, it would have been scrapped and replaced with a new part.

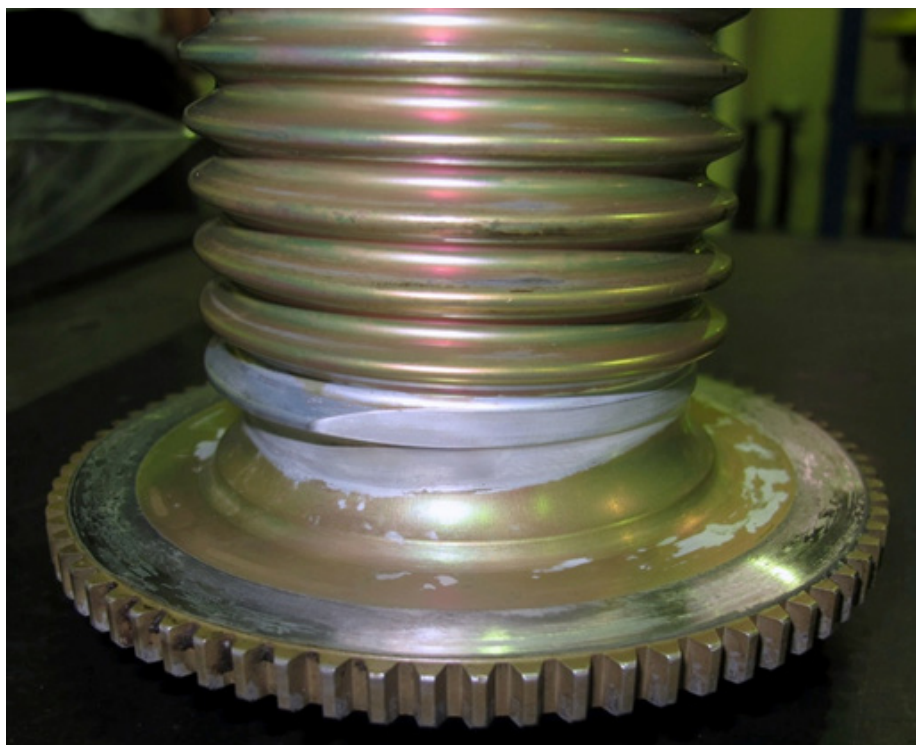


Figure 15: discoloration visible on bolt no.3



Figure 16: through-cavities and machining striation on the side of a bolt (bolt no.1)

1.3.3.3 Examination of the blade bearings of the left propeller

Equipment examined

Bearing of blade no.1	Bearing of blade no.2	Bearing of blade no.3	Bearing of blade no.4
TIMKEN	TIMKEN	TIMKEN	TIMKEN
P/N: RA57099Z-1	P/N: RA57099Z-1	P/N: RA57099Z-1	P/N: RA57099Z-1
S/N: 31474 N/R/R/R	S/N: 62811 N/R	S/N: 30978 N/R	S/N: 61861 R/R

The blade bearings enable the rotation of each blade in the propeller hub and thus to change the propeller pitch. A bearing of the same type is shown in figure 17 and figure 18. The bearing consists of several components, as shown in the sectional view in figure 19.



Figure 17: blade bearing



Figure 18: view of the complete blade bearing assembly

The objective of the examination was to determine whether the condition of the blade bearings may have contributed in any way to the loss of blade no.2, or if they could provide information about the assembly of the propeller during the last overhaul.

During the last overhaul performed by Röder Präzision, the 4 blade bearings were replaced. The 4 bearings installed were not new but resulted from repairs (indicated by the presence of the letter 'R' in the serial number).

The bearing of blade no.2 was found only in part, with the spacer, the outer race, the housing and the outer rollers all missing.

The 3 other bearings were completely removed when the propeller was disassembled at PropTech.

In general, the 3 bearings removed (1, 3 and 4) were found with a quantity of grease deemed to meet the specifications of the OHM. After taking samples of the grease and cleaning, the bearings were subject to visual examination in cooperation with a representative of TIMKEN, the bearing manufacturer.

In addition to the damage described below, the bearings showed traces of blooming on some of their raceways. The TIMKEN representative said that the blooming may be a reaction linked to prolonged contact with grease, especially if the grease is a Mobil brand of grease, which was the case here (Mobil Beacon 325). This phenomenon is known to TIMKEN, and has no effect on the behaviour of the bearings.

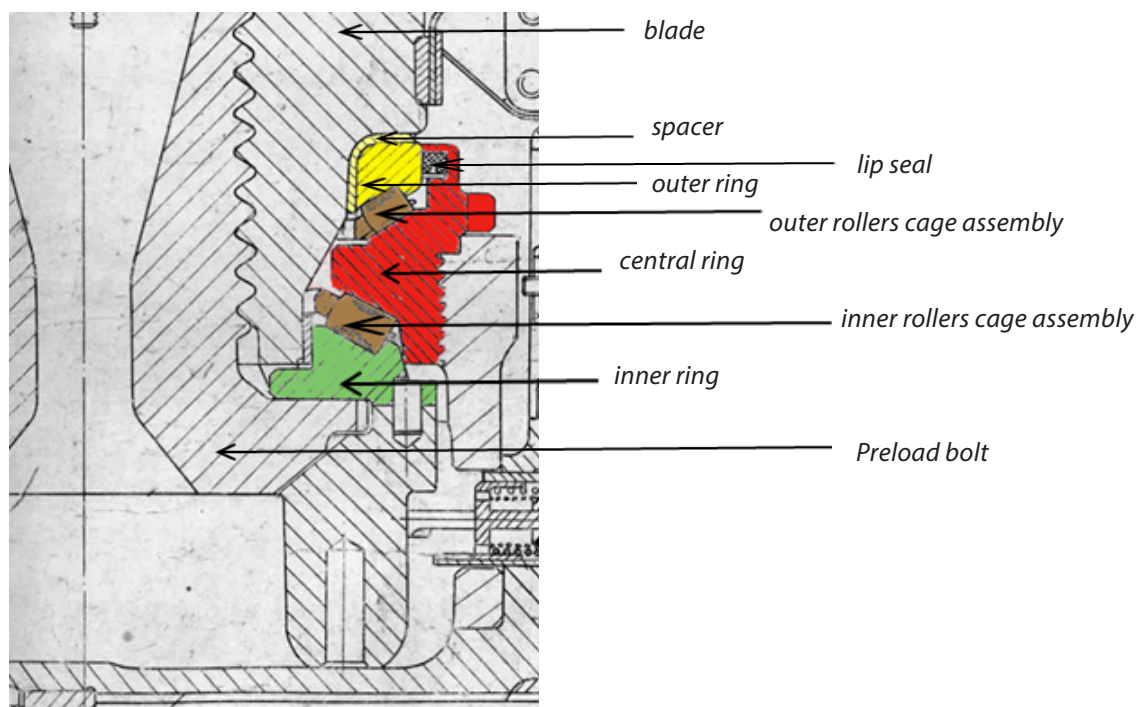


Figure 19 : cross-sectional view of the blade root

1.3.3.3.1 Bearing of blade no.1

The bearing of blade no.1 was severely damaged. The external thread of the central race was torn in places (figure 20) due to the separation of blade no.1 from the hub during its collision with blade no.2 (see § 1.3.3.4) and then with the ground.

All of the outer rollers and cage were destroyed. Some of the rollers were fractured by compression forces. The raceway of the outer ring showed severe indentation. The lower race of the central ring was cracked over its entire circumference and also had severe indentations (figure 21).

The damage was consistent with the shock of blade no.1 against blade no.2 and the separation of blade no.1 from the hub.



Figure 20: external thread torn, central ring



Figure 21: cracking and indentation of the lower race of the central ring

1.3.3.3.2 Bearing of blade no.2

The bearing of blade no.2 was extracted from the hub by the DGA-EP. The significant presence of earth in the lower bearing, as well as traces of surface corrosion were found. After cleaning, the following observations were made:

- ❑ on the central ring, outer side, several areas of surface corrosion and slight contiguous indentation marks, eccentric with respect to the normal position of the rollers on the race;
- ❑ on the lower race of the central ring, the presence of surface corrosion on approximately 180° and contiguous indentation marks spaced from the roller pitch over approximately 130° . This area was located opposite the incipient crack area of the bolt;
- ❑ on the inner rollers, traces of surface corrosion and slight indentation marks and very occasional spalling;
- ❑ on the race of the lower ring, traces of surface corrosion, and a few contiguous indentation marks;
- ❑ a fracture of one sector of the lip seal, which had propagated from the inside of the bearing to outside.

No damage prior to the event could be brought to light. The damage observed was consistent with the separation of blade no.2 and the induced loads.

The surface corrosion observed occurred after the event.

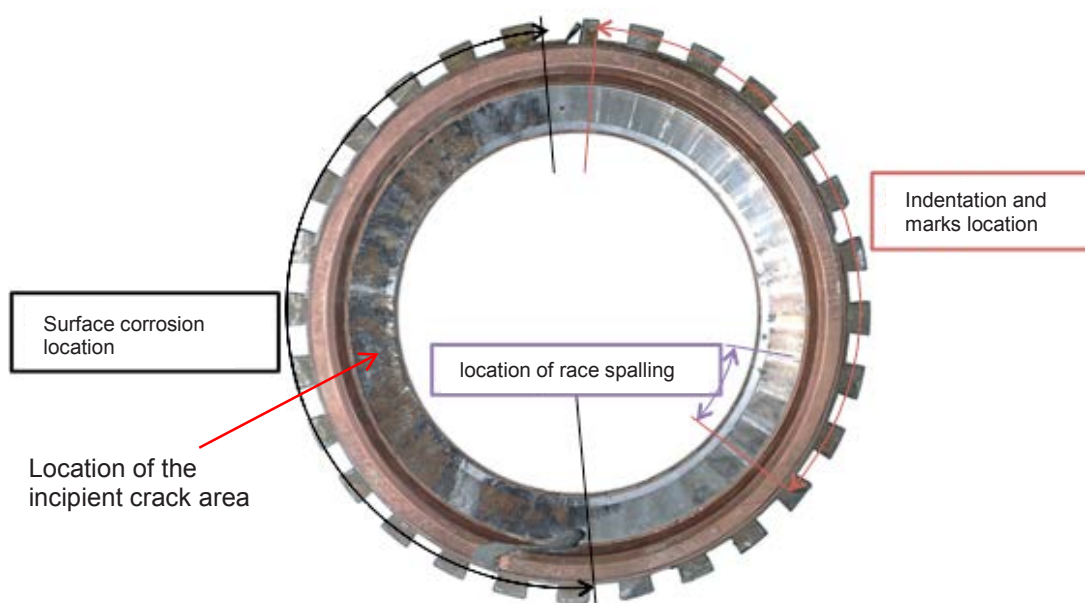


Figure 22: damage found on the outside of the central ring
(Photo DGA-EP)

1.3.3.3.3 Bearing of blade no.3

The general condition of bearing of blade no.3 was found to be correct. However, indentations were observed locally on the lower race of the central ring, outside the raceway (figure 23).

These marks may be related to the impact of the propeller with the ground.

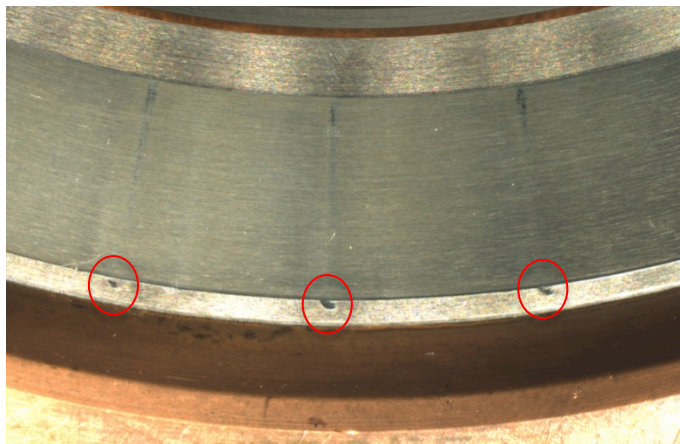


Figure 23 : indentation of the lower race of the central ring

1.3.3.3.4 Bearing of blade no.4

The bearing of blade no.4 had relatively large indentations (brinelling), especially on the races of the upper bearing (figure 24). According to the manufacturer's representative, an aeroplane cannot fly if the bearing of one of its propeller blades has brinelling of this size, which would cause problems controlling the propeller pitch. The marks were therefore more likely to be consecutive to the event, in particular to the shock of the propeller with the ground.



Figure 24: Severe brinelling and traces of blooming on the raceway of the outer ring

1.3.3.3.5 Grease analysis

A sample of grease was taken from bearing nos.1, 3 and 4 during their removal. A sample of the earth found on the bearing of blade no.2 was also taken.

The samples were sent to the DGA-EP for examination. The objective was to ensure that the grease used was compliant with the manufacturer's recommendations.

The OHM specifies the type of grease that can be used for each component. In the case of the bearings, the following greases are allowed:

- AeroShell 7
- Petrofina B2590
- Texaco Lowtep EP
- Mobil Beacon 325

The manufacturer also recommends the use of an anti-fretting paste to be applied on the races of the bearing, called 'FRIN'.

The results of the examination are detailed in DGA-EP report no.54-DAI-13.

They highlight the presence of Mobil Beacon 325 grease, identified in the 4 samples.

They highlight the presence of Mobil Beacon 325 grease, identified in the 4 samples.

Additional tests using X-ray fluorescence spectrometry and observations at x50 magnification after washing revealed the presence of FRIN in samples of grease taken from bearing nos.1, 3 and 4. The amount of earth taken from bearing no.2 proved insufficient to determine the presence of FRIN in bearing no.2.

1.3.3.3.6 Conclusion

The bearings had a wear rate consistent with their use and the number of flight hours after an overhaul. In addition to the normal wear, damage consecutive to the event was observed.

The bearings were lubricated with a grease compliant with the manufacturer's recommendations. The anti-fretting paste (FRIN) was detected in samples from the bearings of blade nos.1, 3 and 4. It was not possible to determine whether FRIN was present in the bearing of blade no.2.

1.3.3.4 Examination of blade no.1

Blade no.1 was found detached from the left propeller. Only the de-icing wire still linked the blade to the hub of the propeller.

The first observations showed that the thread used to attach the blade in the hub was damaged (see §1.3.3.3.1- Bearing of blade no.1 - figure 25 and Figure 26).



Figure 25: no.1 blade alone, after cutting the de-icing wire



Figure 26: root of blade no.1 - damaged thread



Figure 27: bending and twisting deformation of blade no.1

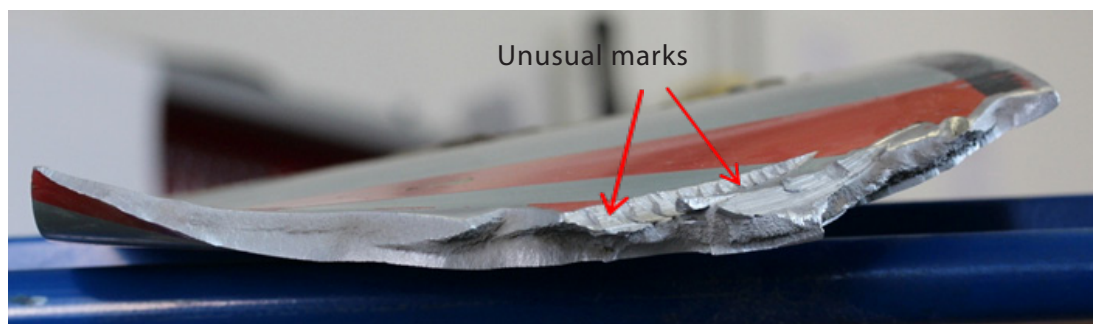


Figure 28: fracture zone at the tip of blade no.1 and unusual marks

The blade has been subject to bending and twisting deformation, and its tip (approximately 150 to 200 mm in length) was missing (figure 27). The fracture of the blade tip was sudden and ductile in nature (granular fracture surface). The clean appearance of the fracture was noted (no earth). There were unusual marks near the fracture area, on the pressure side (figure 28). These marks indicated that blade no.1 hit blade no.2 after the latter broke. This was because the marks corresponded to an impact with the serration of a blade root (figure 29). In addition the serration of blade no.2 was damaged and the geometric matching of the serration with the marks of blade no.1 confirmed this hypothesis (figure 30). The deformations of blade no.1 and the fracture of the tip were therefore consecutive to this impact. An illustrative diagram of the sequence is proposed in figure 31.



Figure 29: marking of the pressure face of blade no.1 in the vicinity of the fracture



Figure 30: damaged serration at the root of blade no.2

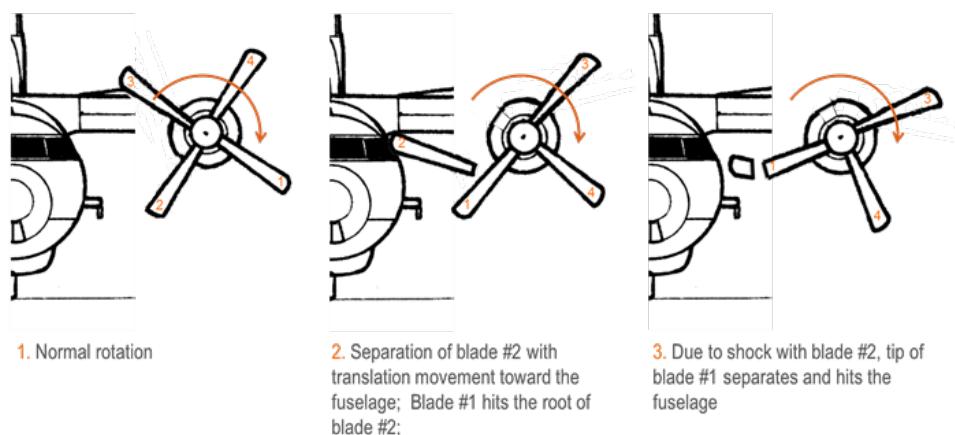


Figure 31: descriptive diagram of the blade loss sequence

The damage observed on blade no.1 is consistent with a tearing of the blade from the hub at the time of the impact with blade no.2, and then with the ground.

1.3.3.5 Examination of blade no.2 and its preload bolt

1.3.3.5.1 Examination of blade no.2

Blade no.2 was found in a field (figure 1). The blade tip was slightly bent towards the pressure side. The leading edge was damaged in several places (figure 32). One part of the damage was particularly pronounced, its shape being curved. It extended from the leading edge to the pressure side and the upper surface. The end of the leading edge was bent towards the rear (figure 36).

The elastomer of the de-icing system had radial cracks along the leading edge (figure 33). Its base had peeled off from the blade. The upper surface had several curved scratches (figure 34). The trailing edge also showed signs of impacts and scratches (figure 35). The pressure side had scratches, two of which were deeper than the others, one at the tip of the blade (approximately 8 cm in length, Figure 36), and the other near the blade root (3 cm long).

Part of the blade root was missing.

The damage and marks on blade no.2 were consistent with a penetration of the blade into the fuselage after its separation from the left propeller. According to the curvature of the scratches, the blade was both translating along its longitudinal axis and rotating.

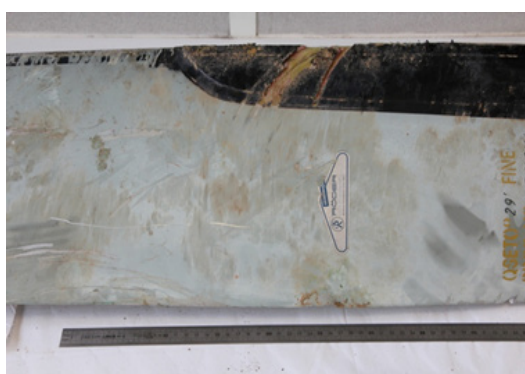


Figure 32: severe damage on the leading edge

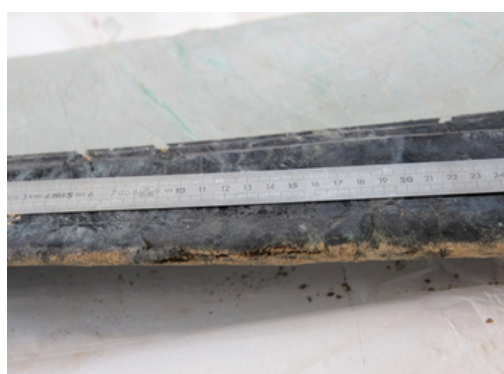


Figure 33: radial cracks in the elastomer of the de-icing system



Figure 34: curved scratches on the upper surface



Figure 35: traces of impacts on the trailing edge

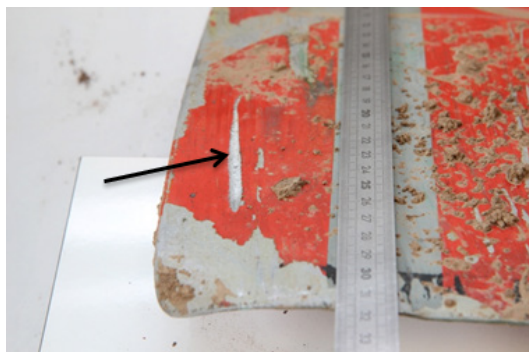


Figure 36: deep scratch on the pressure side



Figure 37: fracture surface of the preload bolt showing signs of fatigue

1.3.3.5.2 Fractographic examination of the preload bolt

The fracture surface of the preload bolt (figure 37) was extracted from the blade by cutting then cleaned with ethanol. The fracture surface was located 8.7 mm under the bolt head (figure 38) in the fillet.

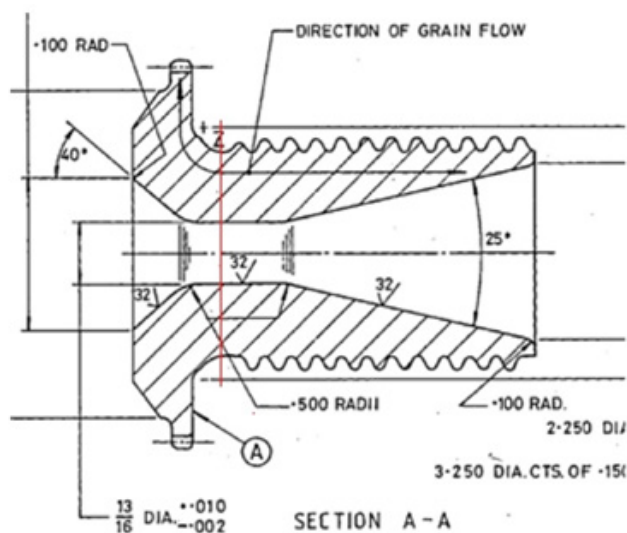


Figure 38: fracture section of the bolt (in red)

The fractographic examination of the rupture surface highlighted two distinct areas (figure 39 to figure 41):

- ❑ a raised granular area, characteristic of a sudden ductile fracture (approximately 60% of the total cross-section);
- ❑ a smooth flat area, with beach marks (or stop marks) and two radial lines (approximately 40% of the total area). These elements were characteristic of the propagation of one (or more) crack(s) under cyclic loading (fatigue crack propagation).

In addition, zones of darker colouring were observed. The first was in the main initiation area of fatigue cracking. The other two were further away from the edge of the part and appeared to extend over one or more stop mark(s).

Observation of the (concentric) stop marks made it possible to determine the crack initiation site figure 40). It was located on the leading edge (figure 42). The presence of two radial lines suggested that two secondary cracks were also initiated and propagated.

Detailed examinations with a scanning electron microscope (SEM) confirmed the presence of a fatigue crack propagation zone, with the presence of fatigue striations (figure 44). The area with high relief had many dimples, characteristic of a sudden ductile fracture (figure 45).

Counting the crack beach marks can provide information on the duration and the propagation speed of the crack. If we consider that each beach mark corresponds to a «*crack opening and closing*» cycle, it can be related to a cycle in which the part is subject to high and low stress loads.

Thus, after counting the beach marks on the whole of the fatigue fracture zone, it was found that (Figure 43):

- ❑ 40 beach marks could be counted between the incipient crack (line concentricity area) and the first dark area, covering 70% of the area. Of the remaining 30%, close to the initiation area, the information was degraded by the openings and re-closings of the crack;
- ❑ 15 beach marks could be counted between the two areas of dark colour;
- ❑ 25 beach marks could be counted between the second area of dark colour and final fracture zone.



Figure 39: fracture surface of preload bolt no.2



Figure 40: detail of the fracture surface, at the initiation site

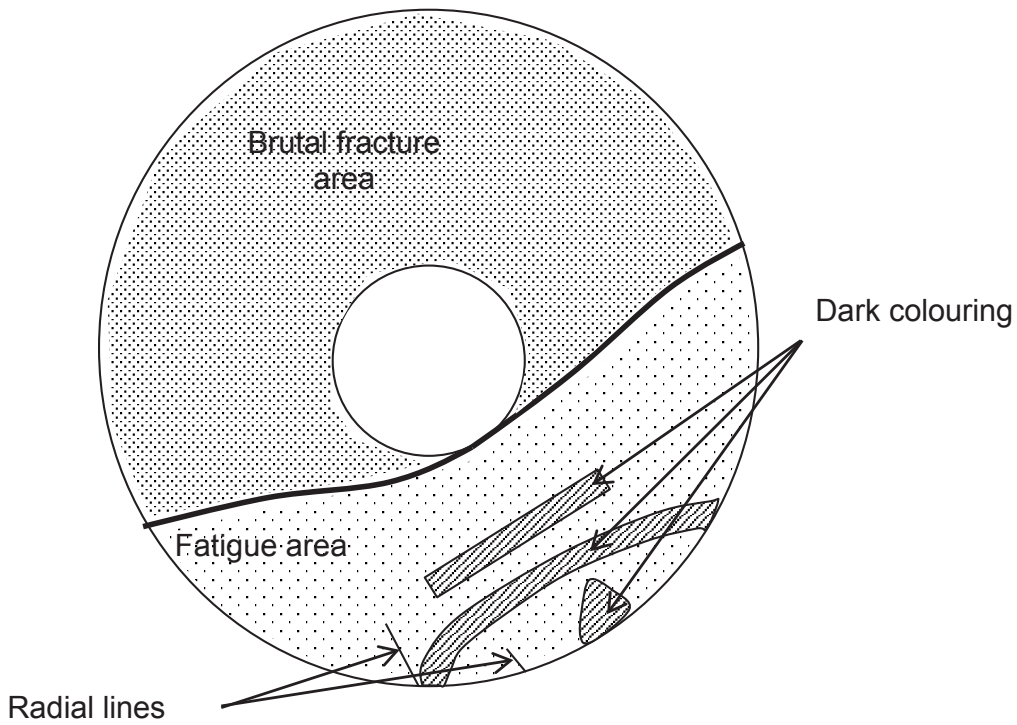


Figure 41: fractographic description of the fracture surface of the preload bolt of blade no.2

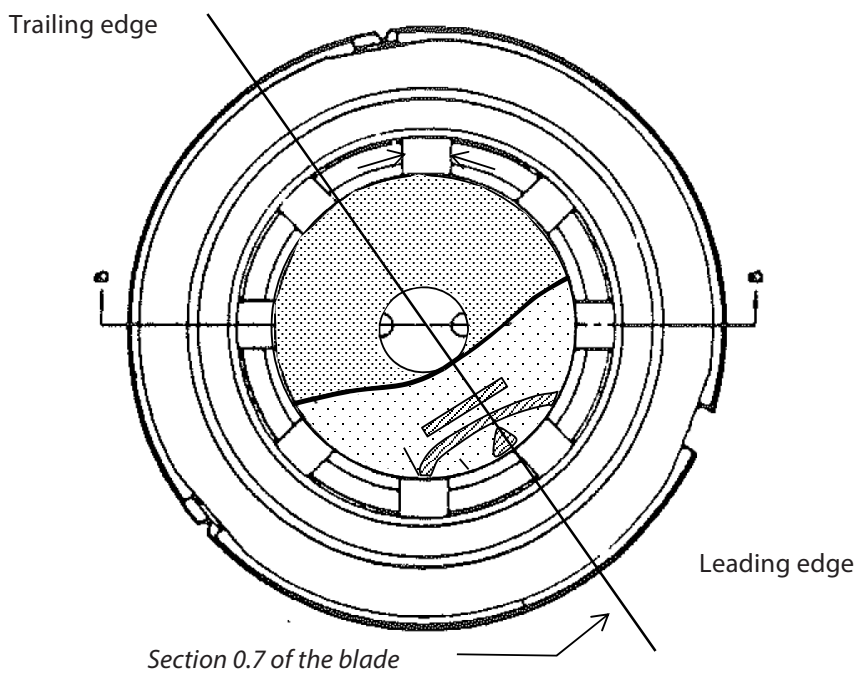


Figure 42 : View of the position of the fracture surface with respect to the blade (bottom view)⁽³⁾

⁽³⁾Section 0.7 of the blade was the section at a distance from the centre of the hub corresponding to 70% of the distance between the centre of the hub and the tip of the blade. A line of paint on the blade was used to locate it. The angle of the propeller pitch was given at this section.

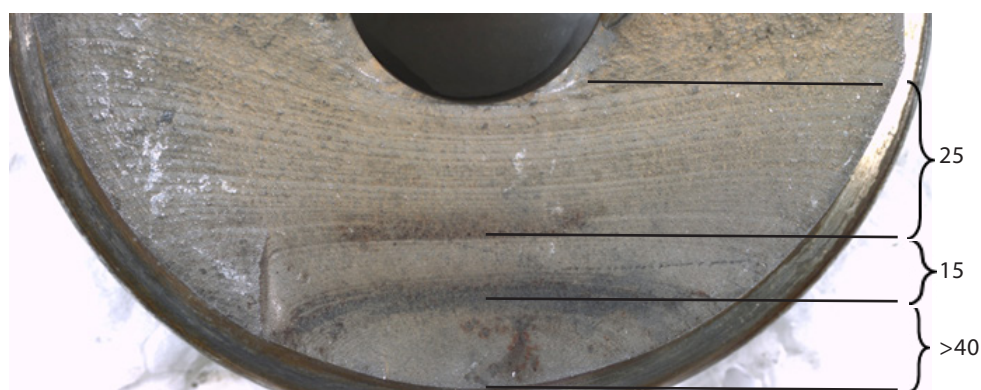


Figure 43 : Overview of fatigue macro-striations - number of beach marks per area



Figure 44: striations in the fatigue area, SEM views

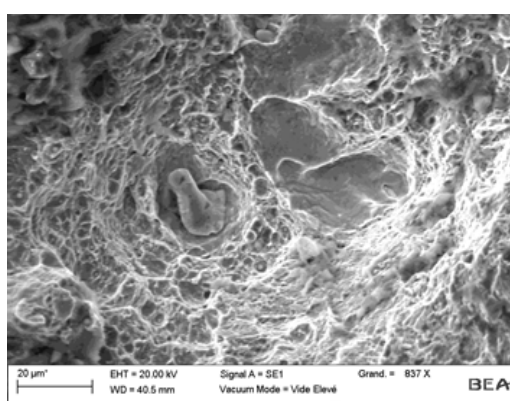


Figure 45: dimples in the final fracture zone, SEM views

Thanks to the fractographic observations it was possible to identify three characteristic zones. These areas are referenced in Figure 46. Area A1 corresponds to the main initiation site of the fatigue crack. Areas A2 and A3 are located near the two radial lines (or ridges), which are secondary crack initiation areas.

Area A1

SEM observations of area A1 highlighted a main crack initiation area, the morphology of which differed from the rest of the fracture surface (figure 47). The main crack initiation area, approximately covering a semi-circle of 100 µm in diameter, had a fracture surface with local porosities (figure 48). Traces of cadmium were also visible locally.

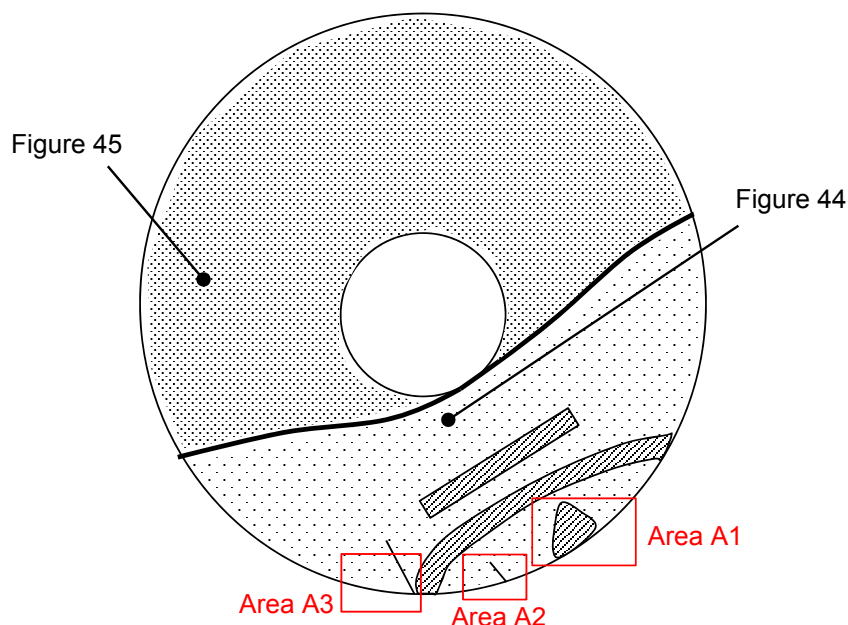


Figure 46 : Areas examined by SEM

At the level of area A1 on the side of the bolt, the absence of cadmium was noted along the fracture surface to a height of approximately 60 μm . The presence of an inclusion was also noted at approximately 100 μm from the fracture surface (figure 51). Chemical analysis by Energy-Dispersive Spectroscopy (EDS) was used to determine the nature of the inclusion: it is manganese sulphide (MnS).

In addition, on the flank of the bolt, numerous through-cavities were observed (figure 49) and even cracks, as illustrated in figure 50.

No pre-damage (tool marks, machining defects, etc.), corrosion pitting or geometric defect was detected at the level of the main crack initiation area.

Area A2

The surface of area A2 showed signs of fatigue cracking. The presence of a radial line (or ridge), suggested that the propagation of the fatigue crack occurred in a plane different from that of the main crack.

An area on the edge of the part was similar to the initiation area of the main crack, with the presence of inclusions (manganese sulphide), and surface porosities (figure 53). No pre-damage (tool mark, machining defect, etc.), corrosion pitting or geometric defect was visible.

Area A3

Area A3 also had a fatigue fracture surface, on which the striations were easily visible (Figure 54). The presence of a ridge line again suggested crack propagation in a plane different from the neighbouring plane (plane of the secondary crack). This is clearly illustrated in Figure 55, which shows the fracture surface of the bolt and the crack extending under this surface.

The initiation site of the tertiary crack could not be identified. No pre-damage (tool mark, machining defect, etc.), corrosion pitting or geometric defect was observed in this area.

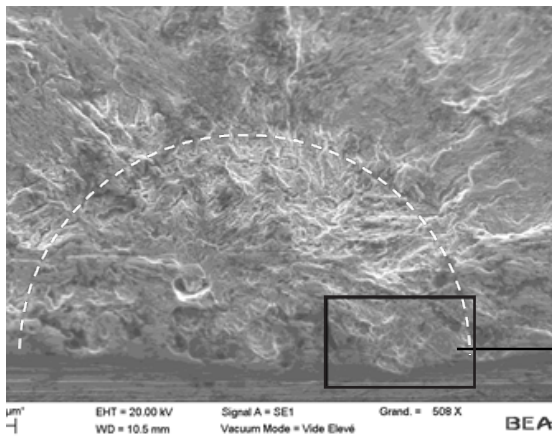


Figure 47: morphology of the main crack initiation area

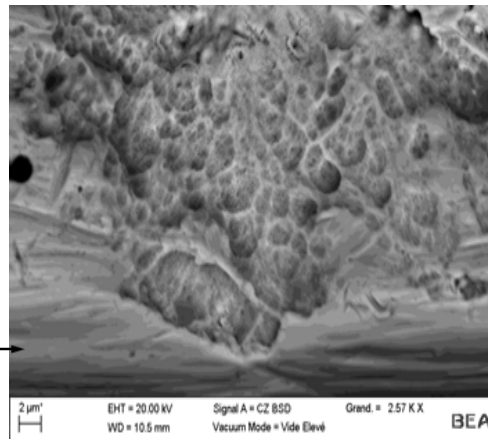


Figure 48: porosities in the main crack initiation area (detail of Figure 47)

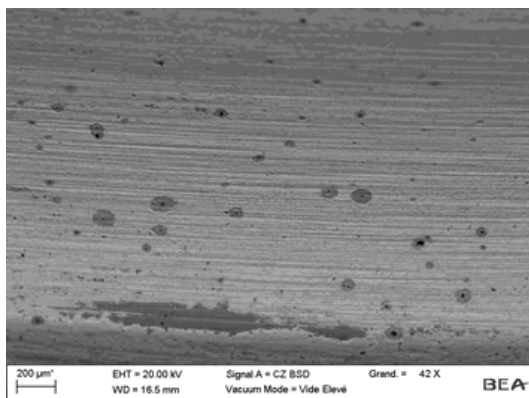


Figure 49: through-cavities on the side of the bolt

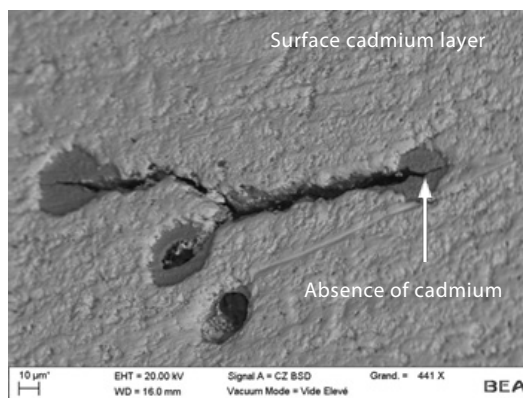


Figure 50: cavities and crack on the side of the bolt

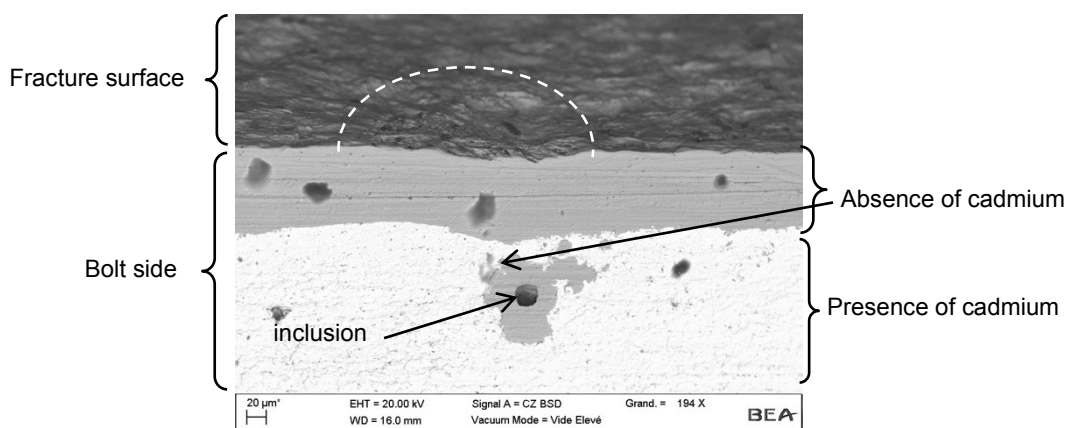


Figure 51: inclusion visible on the side, approximately 100 µm from the fracture surface

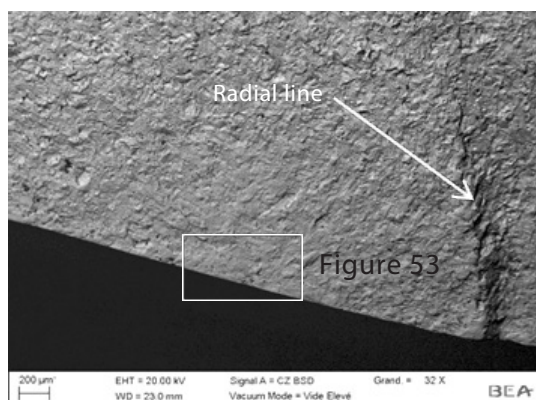


Figure 52: Overview of area A2 by SEM

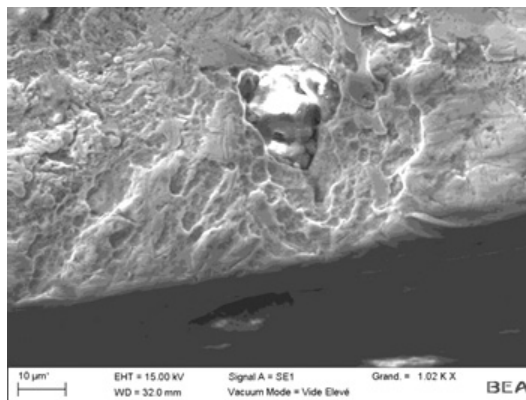


Figure 53 : detail of Figure 52 - porosities on the surface and presence of inclusions

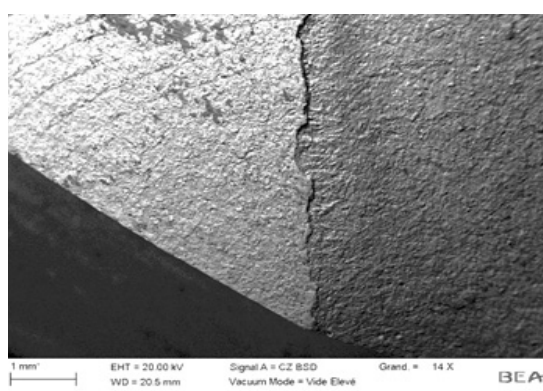


Figure 54: Overview of area A3 by SEM

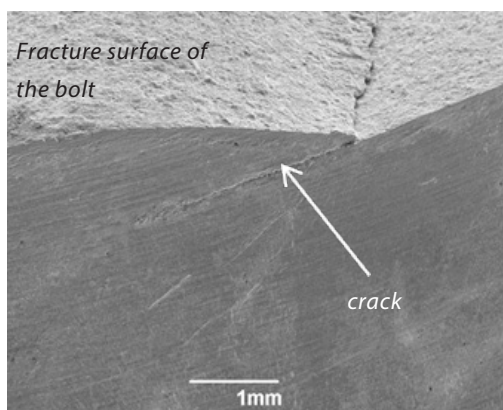


Figure 55: area A3 – matching part of the bolt Figure 54 (Photo DGA-EP)

After these examinations, several metallographic cross-sections were made in order to:

- ❑ characterize in detail the different crack initiation sites;
- ❑ characterize the material the bolt was made of, in particular: the chemical nature of the material (by electric spark spectrometry and by carbon/sulphur titration), its core microstructure, hardness, morphology and composition of the surface coating, as well as the shape and distribution of inclusions.

1.3.3.6 Metallographic inspection

Bolt no.2 (broken)

The location of the cross-sections made on bolt no.2 (referenced C1 and C2) is shown in Figure 56.

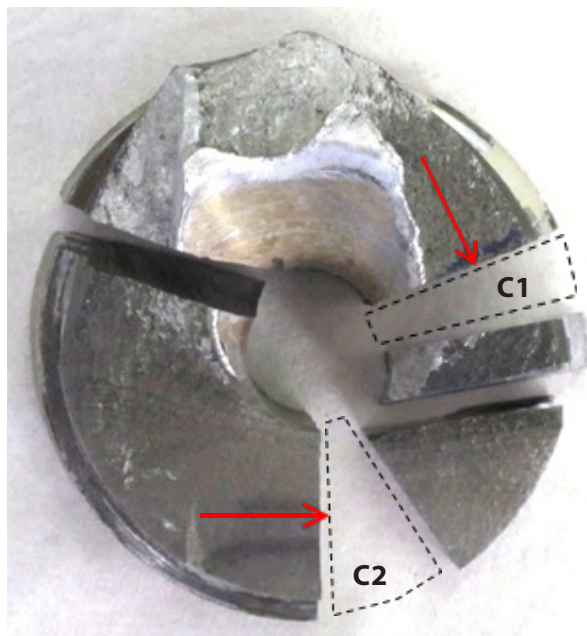


Figure 56: fracture surface of bolt no.2 after cross-sectioning and sampling—red arrow indicates the direction of observation

Cross-section C1 was made in the ductile brutal fracture zone (final rupture).

An examination of the cross-section by SEM and an EDS analysis highlighted the presence of manganese sulphide inclusions (Figure 57). The observation of another inclusion after probable sulphide shedding due to the polishing of the cross-section shows the same type of surface porosities as those observed in the crack initiation sites, as shown in Figure 58.

Observation of cross-section C1 by inverted microscope identified the presence of the surface layer of cadmium, approximately 5 μm thick (Figure 59), for a specification of 0.0003 maximum, i.e. 7.62 μm (manufacturer's drawing). It also appeared that some of these sulphides opened out onto the surface of the part (bolt side). Sulphide shedding then left cavities on the surface of the part (Figure 61, Figure 62, Figure 63).

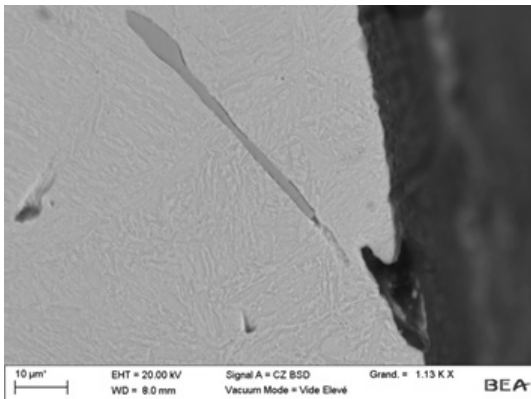


Figure 57: filiform manganese sulphide and surface cavity

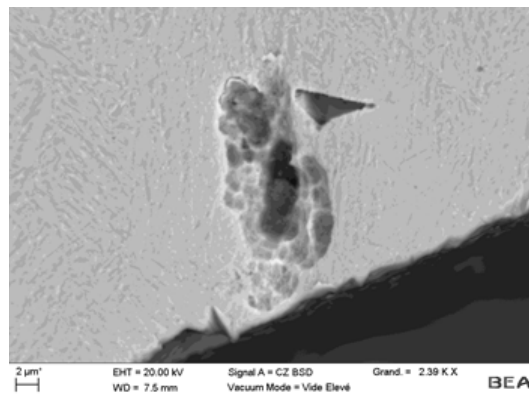


Figure 58: cross-sectional view of a cavity after sulphide shedding

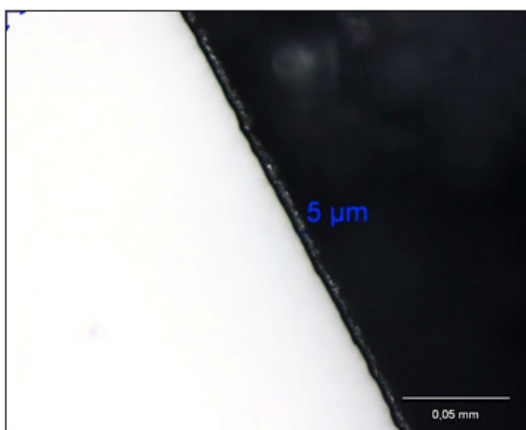


Figure 59: cross-section of the thread root, presence of the layer of cadmium (cross-section C1)

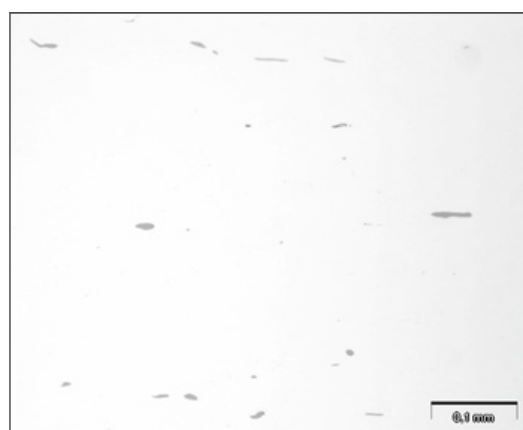


Figure 60: manganese sulphide inclusions in grey (cross-section C1)

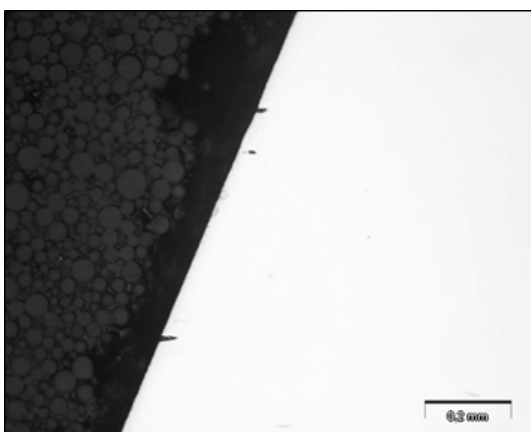


Figure 61: Surface cavities related to manganese sulphide shedding (cross-section C1)

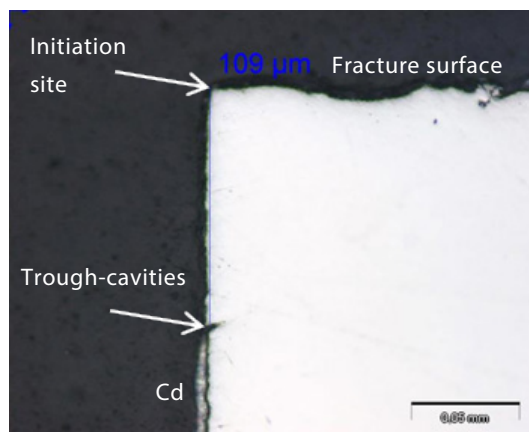


Figure 62: cross-section at the level of the main initiation area (cross-section C2)

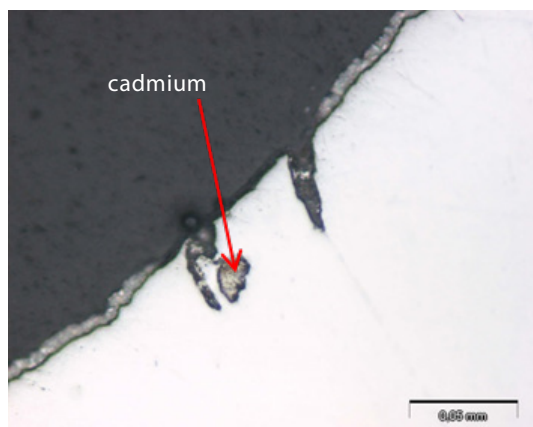


Figure 63: through-cavities with the presence of cadmium at the cavity bottom

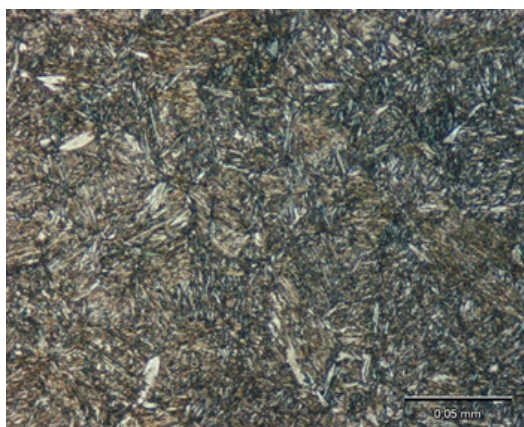


Figure 64: core microstructure: martensite

Cross-section C2, performed in the main fatigue crack initiation site (Area A1), highlighted the absence of the cadmium layer over a hundred μm at the level of the fracture surface. A cavity opening out onto the surface, approximately ten μm deep, was also visible 109 μm below the incipient crack (Figure 62). However, no singularity was observable at the level of the initiation site.

Cadmium could be seen at the bottom of some of the through-cavities. This might be a sign of cadmium plating performed when the cavity was already present and the sulphide had been shed (Figure 63).

Both cross-sections were etched using 2% Nital.

The etchant was used first of all to reveal the grain flow of the steel. The grain flow is caused by the forging of the part. It is specified on the «*direction of grain flow*» drawing in Figure 65. An optimal compromise must be found between the loading of the part and the manufacturing process, so that the grain flow is oriented as much as possible in the direction of stress.



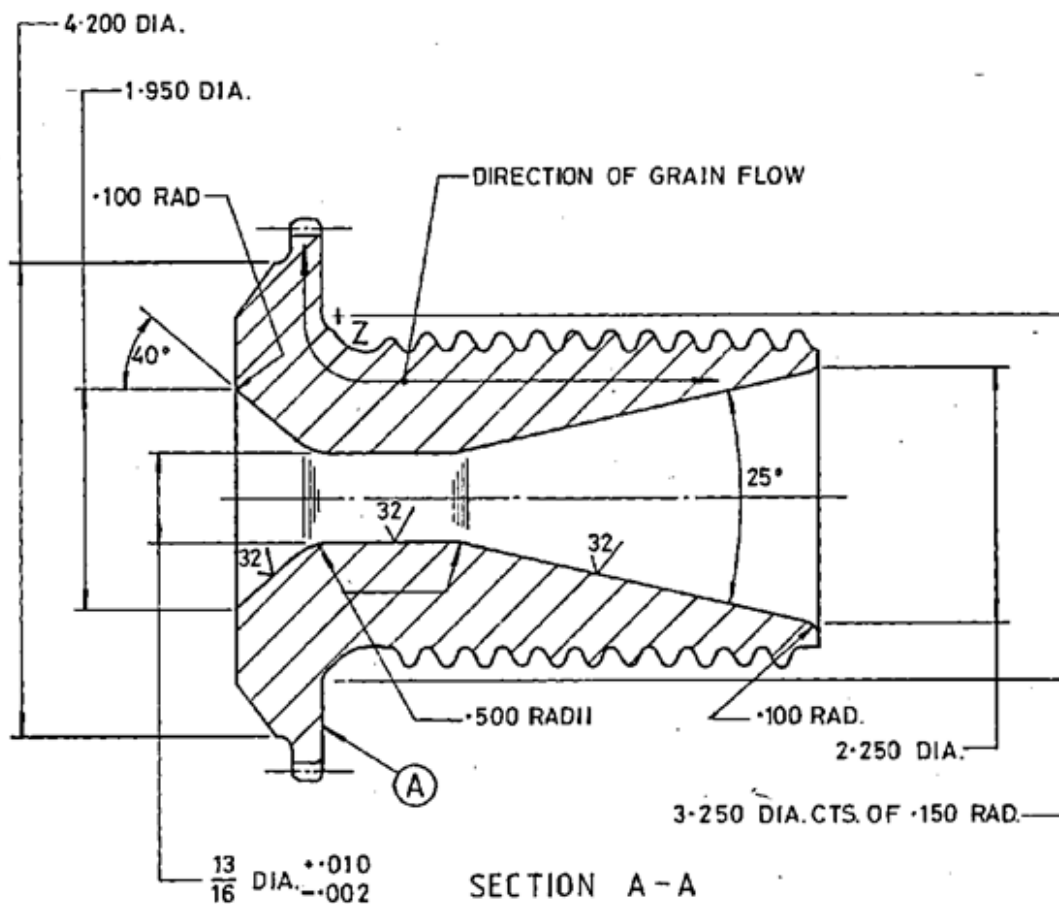


Figure 65: drawing of the preload bolt, longitudinal cross-sectional view

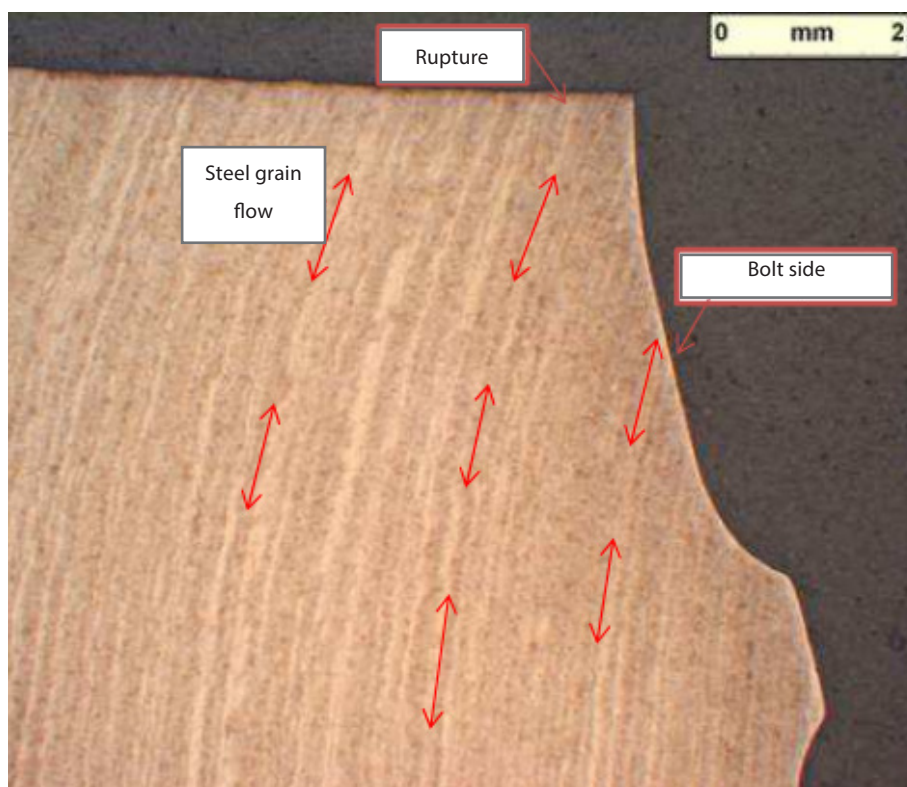


Figure 66: View of grain flow of steel in bolt no.2 in the fracture zone. 90° clockwise rotation of box in Figure 65 (photo DGA-EP)

The grain flow of the steel was consistent with the specification in the drawing. It was noted that the grain flow opened out onto the surface in the fracture zone, at an angle of approximately 30°. This phenomenon was a consequence of the forging and machining operations of the part.

The etchant then revealed the metallographic structure of the steel, in this case a martensitic structure characteristic of quench-tempered steel (Figure 64).

Bolt no.1

In order to have elements for comparison, cross-section examinations were performed on the bolt of blade no.1, as per Figure 67.

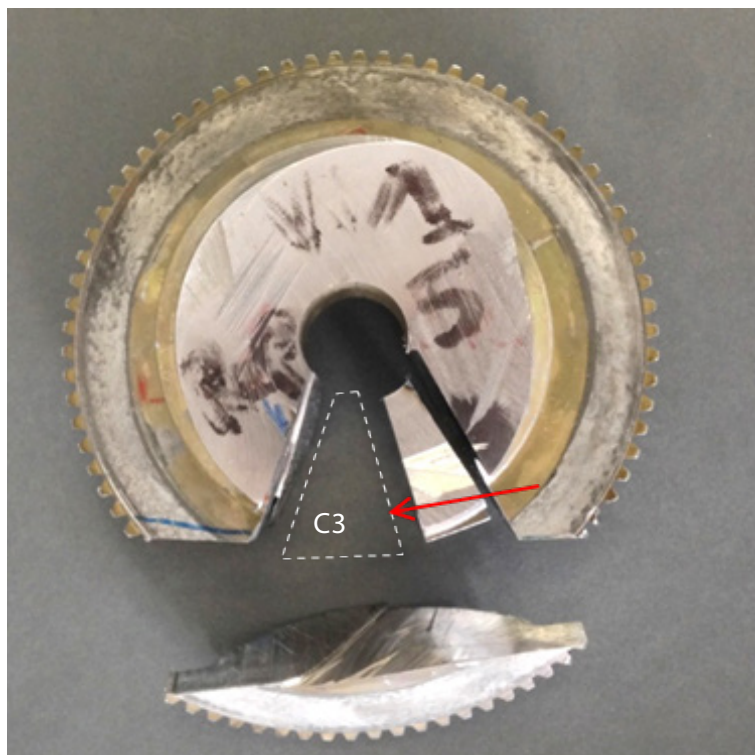


Figure 67: cross-sections of bolt no.1 - red arrow indicates observed face

The grain flow is similar to that of bolt no.2. In Figure 68 it is easier to see the “through” character of the grain flow in the radius of the fracture area of bolt no. 2.

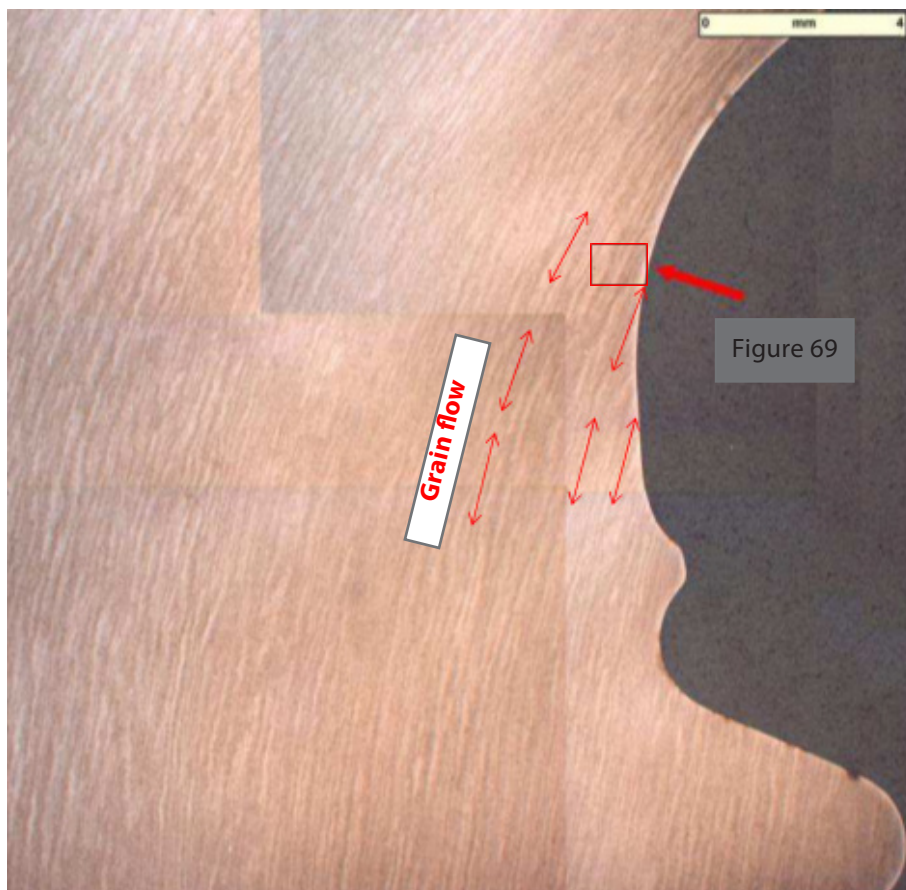


Figure 68: View of grain flow in bolt no.1 in the radius area (fracture zone of bolt no.2)
90° clockwise rotation of box in Figure 65 (photo DGA-EP)

It was seen that the cadmium layer was approximately 6 μm thick. The drawing specified a maximum thickness of 7.62 μm (0.0003 in). Manganese sulphide inclusions could be seen in similar proportions to bolt no.1 (APPENDIX 2). However, when observing a surface cavity, it was noted that a crack approximately 40 μm long had initiated in this cavity, as illustrated in Figure 69. This crack was observed in a plane of the part similar to the fracture plane of bolt no.2.

Magnetic particle inspection is a non-destructive means of inspection used to detect through-defects on the surface or very close to the surface. During the magnetic particle inspection of bolt no.1, this crack was not identified.

The document describing the criticality of the indications observed by magnetic particle inspection is specification NDT2DAP-SPM (Dowty Propellers Standard Practice Manual). According to this document, Aircraft Grade S99 Steel is classified in class 2 and as a result, an isolated inclusion of a length less than 2 mm should be ignored.



Figure 69: crack initiated in a surface cavity (detail of the box Figure 68) - Photo DGA-EP

1.3.3.7 Hardness measurements

Vickers core hardness measurements, under a load of 30 kgf according to NF EN ISO 6507-1 were performed on cross-section C1 (Figure 70). The results, shown in Table 4, complied with the specifications for Aircraft Grade S99 Steel.



Figure 70: references for hardness measurements

References	Hardness HV
Reference 1	420
Reference 2	417
Reference 3	416
Reference 4	410
Reference 5	412
Reference 6	418
Average	416
S99 specification	380-435

Tableau 4: Hardness test results

Hardness measurements using the same method were carried out on a sample from the bolt of blade no.1. The mean value obtained, 407 HV30, was in accordance with the specifications.

1.3.3.8 Chemical analysis

Analyses of the material were carried out on the fracture surface of blade bolt no.2, by Energy-Dispersive Spectroscopy (EDS) coupled to the SEM.

These analyses showed that:

- the dark areas were areas containing high levels of oxygen (O). They were areas with high levels of oxides;
- traces of cadmium were found in the main crack initiation area on the fracture surface, as well as in the secondary crack initiation area;
- cadmium was found in some through-cavities emerging on the surface.

Analyses by electric spark spectrometry and infrared spectroscopy (confirmation by carbon/sulphur titration) were used to determine the chemical composition of samples taken from bolts 1, 2, 3 and 4. The results are given as a mass fraction (%w) in Table 5.

It was observed that the chemical composition of bolt nos. 1, 3 and 4 corresponded (as far as the measurements are concerned) to the specifications for S99 steel. As to bolt no.2, the weight percentages of C and S were slightly superior to those specified and the weight percentage of Mn was very slightly greater than or equal to the limit of the maximum value specified. Moreover, the sulphur content of bolt no.2 was 1.6 to 1.9 times higher than that of bolt nos. 1, 3 and 4⁽⁴⁾.

Sample	C %w	Mn %w	P %w	S %w	Si %w	Ni %w	Cr %w	Mo %w	Al %w
S99 specification	0.36 – 0.44	0.45 – 0.70	Max 0.025	Max 0.020	0.10 – 0.35	2.3 – 2.8	0.5 – 0.8	0.45- 0.65	0.015-0.050
Bolt no.1, radius	0.38-0.44	0.68	0.023	0.011-0.015	0.31	2.58	0.66	0.56	Not detected
Bolt no.2, bolt head	0.44-0.46	0.71	0.021	0.020-0.024	0.26	2.61	0.74	0.52	Not detected
Bolt no.2, radius, near A1	0.44-0.48	0.69	0.021	0.020-0.026	0.25	2.61	0.74	0.53	Not detected
Bolt no.3, bolt head	0.38-0.44	Not measured	Not measured	0.009-0.015	Not measured	Not measured	Not measured	Not measured	Not measured
Bolt no.4, bolt head	0.38-0.44	Not measured	Not measured	0.009-0.015	Not measured	Not measured	Not measured	Not measured	Not measured

Table 5: composition by weight percentage of bolt nos. 1, 2, 3 and 4 measured by electric spark spectrometry and infrared spectroscopy

⁽⁴⁾When the result is given as a range, it includes the measurement uncertainty.

1.4 Examination of the right propeller

1.4.1 Purpose of the examination

The purpose of the examination of the right propeller was to characterize the general condition of the propeller and provide elements of comparison with the results of the examinations on the left propeller.

For this reason, the same dismantling and measurement protocol applied to the left propeller was followed. Like the left propeller, the examination took place at Proptech. The examinations took place on 3 and 4 September 2014, with representatives of Proptech, Dowty Propellers and the BEA.

1.4.2 Equipment examined



1.4.3 Results

The propeller was conveyed from Roissy Charles-de-Gaulle Airport (France) to Proptech (United Kingdom) by truck, by the operator.

On site, the examinations started by checking the external appearance of the propeller with a visual inspection. The following was observed:

- the trace of an impact on the leading edge of blade no.1 (already mentioned in §1.1.2 and shown in Figure 71);
- damage to the de-icing system of blade no.2.



Figure 71: impact traces on the blade no.1



Figure 72: damage to the de-icing system of blade no.2

The damage was the sign of mechanical impacts with elements probably ejected from the fuselage when blade no.2 of the left propeller passed through the airframe.

The 4 blades were then removed from the hub, measuring the pitch-change torque for each beforehand. The results of the measurements are shown in Table 6.

Blade no.	Pitch-change torque	Comment
1	90-100 lb.ft	Jerky rotation
2	180 lb.ft	Jerky rotation
3	185-190 lb.ft	Jerky rotation
4	160 lb.ft	Jerky rotation ⁽⁵⁾
<i>OHM* specifications</i>	<i>90-190 lb.ft</i>	<i>Smooth rotation</i>

*For information only, values valid only on assembly

Table 2: pitch-change torque values for the 4 blades of the right propeller

The individually measured values were within the range specified by the OHM. However, it also specifies that two opposite blades must not have pitch change torques that differ by more than 30 lb.ft. Given this criterion, blade no.1 seemed to be off-spec. However, it is important to remember that the leading edge of this blade was damaged and was probably hit.

A yellow product was observed on the pitch-change pin of each blade. During the discussions with the Proptech mechanics, the possibility was mentioned that this product was Titanine JC5A, a material applied as a seal at the interface between different parts of the propeller, in particular at the level of the hub assembly.

The preload bolts were then removed, after first noting the outside diameter of the bearing and the rotation torque of the blade. Once the bolts had been removed, the diameter of the bearing was once again measured. The difference between the two diameters of the bearing was compared with the range of expansion values on assembly, specified in OHM. The results are shown in Table 7. The values in red were outside the specifications of the OHM.

⁽⁵⁾The propeller was stored on the aeroplane involved in the accident between the time of the accident and the time the samples were taken for examination. It never rotated between those two occasions. For this reason, under these conditions it is possible that the blade root bearings, subject to pre-loading during assembly, generated indentation phenomena (brinelling), which may have marked the raceways which may explain the jerky rotation of the blade.

Blade no.	Bearing diameter before removal	Bearing diameter after removal	Difference (shrinkage when negative)	Bearing torque before removal
1	6.4840"	6.4800"	-0.0040"	120 lb.ft
	6.4840"	6.4795"	-0.0045"	
2	6.4840"	6.4795"	-0.0045"	160 lb.ft
	6.4850"	6.4800"	-0.0050"	
3	6.4850"	6.4805"	-0.0045"	180 lb.ft
	6.4865"	6.4810"	-0.0055"	
4	6.4855"	6.4800"	-0.0055"	150 lb.ft
	6.4850"	6.4800"	-0.0050"	
OHM specifications on assembly*	<6.5050"		0.0040" – 0.0045"	90-190 lb.ft

*For information only.

Table 7: values measured on each blade of the right propeller

For each of the blades, several shims were found in abnormal locations, such as outside the blade root fitting on the bolt head (Figure 73). Shims are normally used inside the bolt/bearing assembly as specified in the OHM, and cannot escape. They were probably located there during the assembly of the propeller. Traces of moisture were also observed on the bolt head.

The rotation torque and shrinkage values for the bearing were very close to specifications.

The 4 preload bolts were examined by magnetic particle inspection. These examinations revealed no indication of a defect or crack.

After dismantling, the blade root bearings were examined. They were in good condition and properly greased. Two of the bearings were damaged on one of the raceways, which appeared to be related to the presence of a foreign body temporarily trapped between the race and the rollers (Figure 75). No foreign body however was found during disassembly. The other observations (the surface corrosion in Figure 74, humidity) can be explained by the stationary position of the right propeller on the aeroplane, between the date of the accident and the examination (approximately 9 months).

In conclusion, the only abnormality observed during the examination of the right propeller was the damage present on one of the races of two bearings, the cause of which seemed to be the temporary presence of a foreign body between the race and the rollers. This foreign body was not recovered during dismantling.

The measurements made during disassembly of the propeller show that there had been no loss of the pre-loading of the bearings on the propeller since the last assembly.

The preload bolts were in good condition. The low value of the pitch-change torque measured on blade no.1 can be explained by the fact that it was probably hit by debris from the fuselage after blade no.2 from the left propeller crossed the airframe.



Figure 73: shim found outside the bearing/bolt assembly - traces of moisture

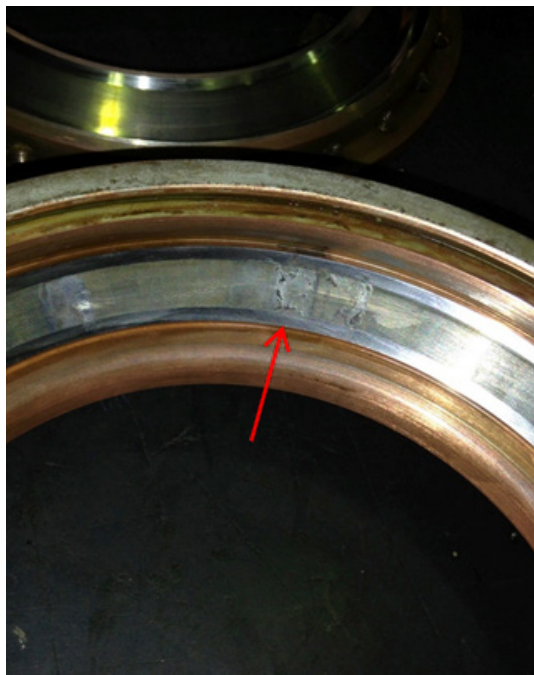


Figure 74: corrosion visible on one of the raceways

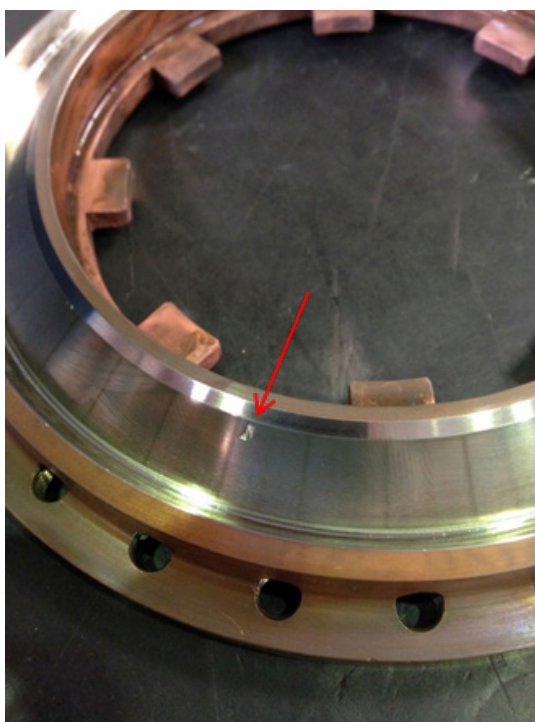


Figure 75: damage to the race of bearing no.2

1.5 Examination of other propellers of R193-type

1.5.1 Purpose of the examination

On 10 March 2014, the operator of the Fokker 27 I-MLVT involved in the accident told the BEA that both propellers of a Fokker 27 belonging to Falcon Express Cargo (United Arab Emirates) and operated by Astral Aviation (Kenya) had to be sent to Piedmont Propulsion Systems, LLC (USA) to undergo an inspection of the blade bearings.

In agreement with the operator, the BEA asked Piedmont to follow the protocol described in §1.3.3.1 on both propellers in order to obtain data from accident-free propellers, for comparison with the results in §1.3.3.1. Grease samples were also collected from the blade bearings of the two propellers. The disassembly, measurements and grease sampling operations were carried out on 3 April 2014.

On 11 March 2014, the operator informed the BEA that it was sending the right propeller of the Fokker 27 registered I-MLRT to Field Airmotive (South Africa) for repair as part of the guarantee covering the overhaul and release to service carried out by Field Airmotive on 28/01/2013. This repair request occurred after an anomaly was detected during the inspection required by Dowty Service Bulletin 61-A1152⁽⁶⁾, published by Dowty on 20/11/2013, i.e. less than one month after the accident.

As before, in agreement with the operator, the BEA asked Field Airmotive to follow the protocol described in §1.3.3.1 and to apply it to the propeller, in order to add elements of comparison with the results obtained during the dismantling operation of the propeller involved in the accident. The operation was carried out in April 2014.

⁽⁶⁾The anomaly was reported as follows: "Blade no.2 extremely rough to turn".

1.5.2 Equipment examined

Propeller	Propeller	Right propeller I-MLRT
Dowty-Propellers P/N: R193/4-30-4/61 S/N: DRG/1608/82	Dowty-Propellers P/N: R193/4-30-4/61 S/N: DRG/2793/83	Dowty-Propellers P/N: R193/4-30-4/61 S/N: DRG/292/66

Further information:

- ❑ DRG/1608/82:
TSN: 18,342 hours
TSO: 2,785 hours
Last overhaul performed by Piedmont on 30/07/2008 at TSN 15,557 hours.
- ❑ DRG/2793/83:
TSN: 22,994 hours
TSO: 1,002 hours
Last overhaul performed by Röder Präzision on 06/01/2008 at TSN 21,992 hours.
- ❑ DRG/292/66:
TSN: 25,455 hours
TSO: 396 hours
Last overhaul performed by Field Airmotive on 28/01/2013 at TSN 25,059 hours.

1.5.3 Results

Due to the fact that the propellers were transported with their blades separated from the hub, the only results that could be compared were the shrinkage values of the bearings after unscrewing the preload bolt. Note that the bearing shrinkage value is the difference between the diameter of the bearing measured before disassembly and the bearing diameter measured once the bearing has been removed.

These data are compiled in Table 8. The values in red are outside the assembly specifications.

	DRG/1608/82	DRG/2793/83	DRG/292/66	Specification*
Blade no.1	0,0040" 0,0040"	0,0051" 0,0052"	N/A	>0,0040" <0,0045"
Blade no.2	0,0041" 0,0040"	0,0026" 0,0023"	0,0030" 0,0030"	
Blade no.3	0,0042" 0,0041"	0,0038" 0,0039"	N/A	
Blade no.4	0,0043" 0,0040"	0,0038" 0,0041"	N/A	

**The value specified in the OHM is actually a range of expansion values measured during assembly. The specification therefore is not directly comparable with the measured shrinkage value.s*

Table 8: shrinkage values of the blade root bearings measured during disassembly

Propeller DRG/1608/82 had values within specification, although the last overhaul had taken place 2,785 flight hours earlier, conducted by Piedmont. For propeller DRG/2793/83, overhauled 1,002 flight hours earlier by Röder, two of the blades had values that were significantly off-spec, and values for two other blades that were very close to specification. Finally, blade no.2 of propeller DRG/292/66, although overhauled only 396 flight hours earlier by Field Airmotive, also had off-spec values.

During the interview with a Piedmont operator, he claimed that from experience, 50% of the bearings arrived for maintenance with pre-load values below the limit values recommended for assembly by the OHM. According to him, the loss of pre-loading may be related to the wear of the bearings, corrosion, aging or a change in distribution of the grease within the bearing, for example. In his opinion, a value of 0.0025" would be an average shrinkage value of the bearings, according to his experience.

Samples of grease were collected from the four bearings of propellers DRG/1608/821 and DRG/2793/83.

Additional examinations by X-ray fluorescence spectrometry and observation at x50 magnification after washing the samples highlighted the presence of FRIN in each of them.

1.6 Additional Information

1.6.1 Previous events

1.6.1.1 Falconair Viscount 784, registered SE-CNL

On 23 July 1967, a Vickers Viscount 784 operated by Falconair registered SE-CNL lost its right propeller as a result of the loss of blade no.1 of the propeller.

The propeller was of the R130/4/20/4/12E type. The blade root technology was similar to that of propeller R193/4-60-4/61 (Figure 76).

According to the Dowty Rotol Ltd. investigation report, the loss of blade no.1 could be attributed to incorrect installation of the centre race seal on the blade root bearing (Figure 76).

The seal was found twisted, allowing moisture to penetrate the bearing, and grease to escape. This resulted in the emergence of severe corrosion pits on the bearing raceways, resulting in a significant loss of the bearing pre-load. Stress in service on the preload bolts was thus significantly increased, causing the fatigue failure of the bolt in the fillet radius under the bolt head.

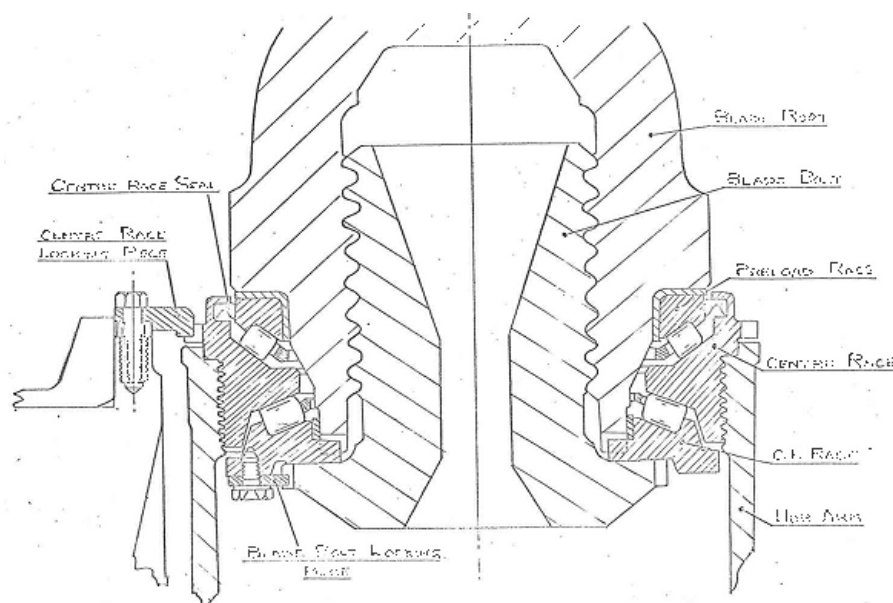


Figure 76 : drawing of the blade root of propeller R130/4-20-4/12E.

Excerpt from the Dowty Rotol Ltd investigation report on the accident involving SE-CNL.

1.6.1.2 Manufacturer's feedback

Dowty Propellers said they had no knowledge of similar events on this type of propeller, except for the event described above.

Dowty were responsible for a significant part of the maintenance operations on these propellers from the late 1950s until the early 1990s, i.e. the main period of their use. Dowty estimated that a total of some 5,400 propellers had been in service. They estimated the number of replacement blades to be approximately 15% of the total, or 817 more. Thus, it would appear that more than 100 million flight hours have been accumulated by this type of propeller.

According to them, the replacement of the preload bolt was a rare occurrence.

1.6.2 Maintenance

1.6.2.1 Aircraft history file

1.1.1.1.1 Left propeller

The last installation, removal or maintenance operations on the left propeller of I-MLVT (S/N DRG142/64) are listed below. In September 2001, the propeller was installed on the left-hand side of F-ZBFG⁽⁷⁾, by EADS Sogerma in Marignane. In October 2002, an overhaul of the propeller was carried out by Technic-Aviation Manosque. Between September 2001 and July 2005, no activity of the propeller was reported in the logbook. From July 2005, activity once again became relatively detailed.

- **July 2005**
 - removal of the propeller from the F-ZBFG for inspection of the blade bearings (TSN: 11,600)
- **February 2006**
 - inspection of the blade bearings by Röder Präzision
- **June 2006**
 - installation of the propeller on the left of I-MLTT⁽⁸⁾
- **March 2009**
 - removal of the propeller from the left of I-MLTT for an overhaul by Röder Präzision (TSN: 12,994)
- **June 2009**
 - o installation of the propeller on the left of I-MLRT⁽⁹⁾
- **August 2012**
 - Removal of the propeller from the left of I-MLRT for convenience (TSN: 14,609)
- **September 2012**
 - Installation of the propeller on the left of I-MLVT
- **June 2013**
 - Removal of the propeller from the left of I-MLVT (TSN: 14,986)
 - Installation of the propeller on the left of I-MLRT
 - Removal of the propeller for repair of the de-icing system on blade no.1 (TSN: 14,997)
- **September 2013**
 - o Installation of the propeller on the left of I-MLVT (TSN: 14,997)

⁽⁷⁾Fokker F27-600 operated by the French Civil Defence authorities.

⁽⁸⁾Fokker F27-500 operated by Miniliner.

⁽⁹⁾Fokker F27-500 operated by Miniliner.

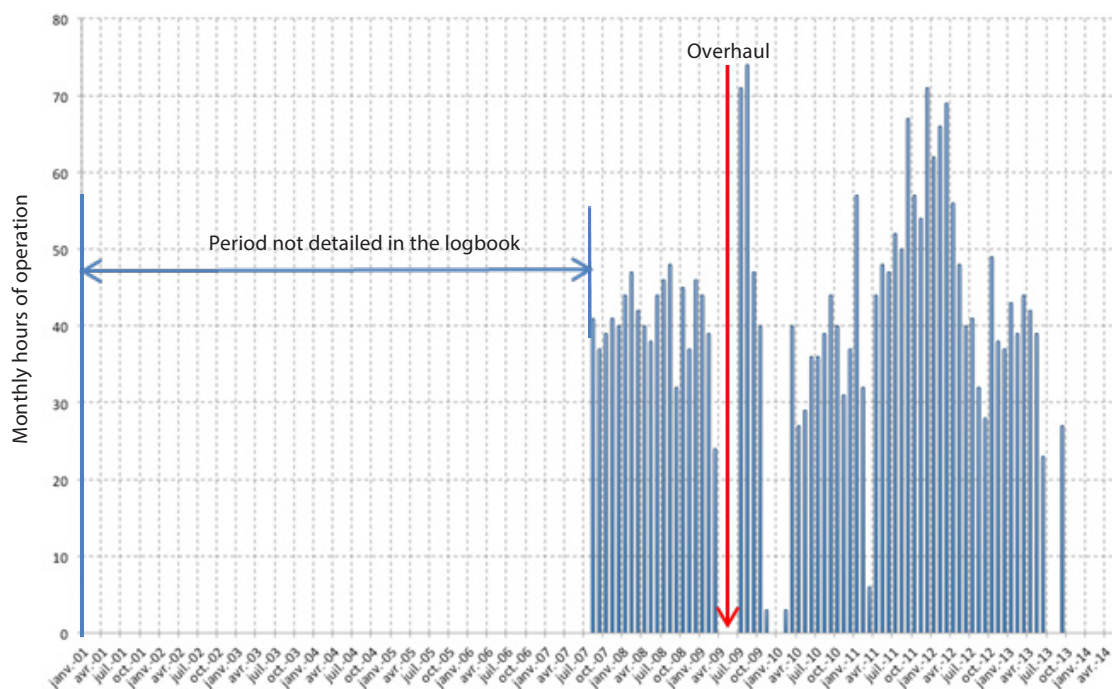


Figure 77: Monthly hours of operation of the left propeller

The propeller maintenance log was also used to trace, from August 2007 to September 2013, the number of monthly hours of operation of the propeller (Figure 77) and at least from January 2001 to September 2013, the cumulative number hours of operation (Figure 78).

The Italian Civil Aviation Authority (ENAC) authorized Miniliner, the operator of Fokker 27 I-MLVT, to follow the schedule specified by Dowty Service Bulletin SB 61-825 for propeller maintenance. This decision was taken in view of the activity of the aircraft, closer to that of a business aeroplane than a commercial transport aeroplane (approximately 30 flight hours per month). The maintenance schedule for business aviation differs from the schedule for commercial transport aviation, specified in SB 61-985.

The Time Between Overhaul (TBO) of the left propeller of I-MLVT was consistent with the schedule for business aviation, specified in SB 61-825.

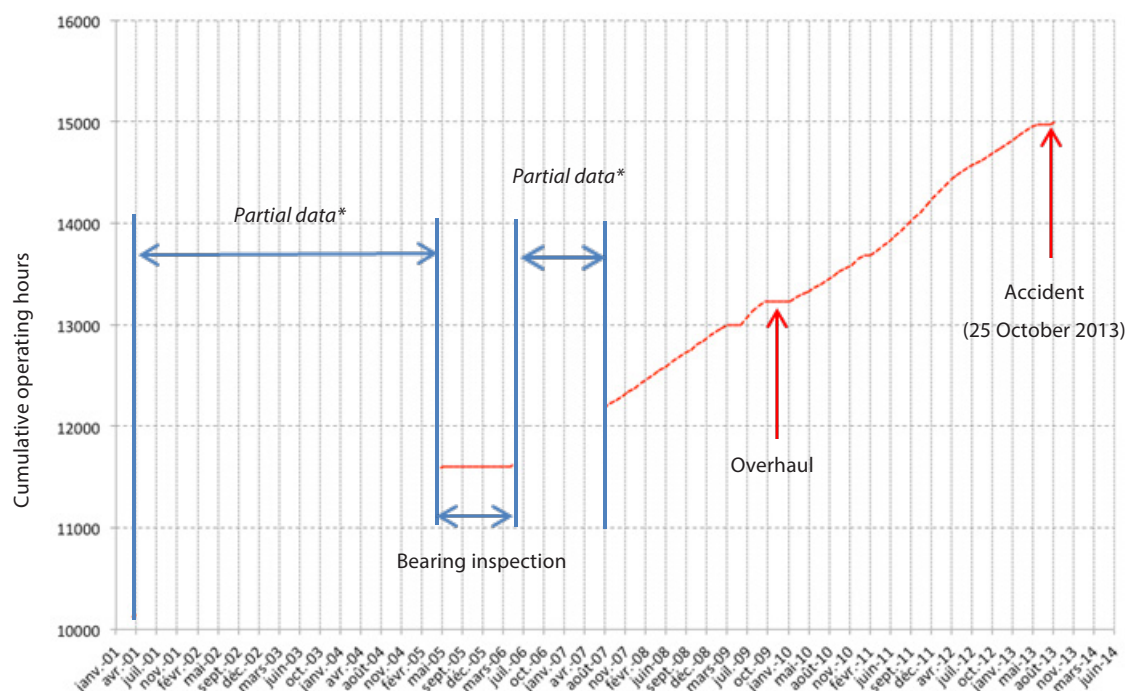
1.1.1.1.2 Right propeller

TSN: 10,780 hours

TSO: 1,617 hours

Last overhaul performed by Röder Präzision on 27/02/2007 at TSN 9,162 hours.

Bearing inspection performed by Piedmont on 20/08/2012 at TSN 10,308. The reassembly of the propeller was made by Proptech, in Italy, on 8/10/2012. The propeller was installed on the right side of I-MLVT on 20/10/2012 and remained there until the date of the accident.



* The data for this time interval is the number of hours of operation of the propeller at the beginning and at the end of the interval.

Figure 78: Cumulative operating time of the left propeller S/N DRG142/64 (in red)

1.6.2.2 Maintenance Documentation

The work cards for the last overhaul carried out on this propeller by Röder Präzision were requested by the BEA.

According to the currently applicable regulations (Part 145.A.55 §M4(c)3), the maintenance documentation must be kept by the maintenance shop for 3 years after the completion of the operations.

The last overhaul of the left propeller of I-MLVT was dated March 2009. Röder Präzision therefore kept the documentation for that maintenance operation for the regulatory 3 years, until March 2012. The company then deleted it. No copy of these maintenance documents was transmitted in advance to the operator or owner of the aircraft. Transmission of the documents is not mandatory, but can be decided spontaneously by some maintenance organizations so that the operator can keep track of maintenance operations.

Röder Präzision decided to stop maintenance of the R193 type of propeller on 06/07/2012.

For this reason, it was not possible to obtain any work cards or detailed maintenance documents for the overhaul of the left propeller (except the return to service certificates provided to the operator and the aeroplane's logbook).

2 - CONCLUSION

The examinations carried out on the various items of equipment on the aircraft involved in the accident made it possible to establish the following facts:

Scenario of the event

- ❑ Shortly after take-off, blade no.2 separated from the left propeller of the Fokker 27 registered I-MLVT. The tip of the follower blade, blade no.1, hit the root of blade no.2, causing the fracture of the tip of blade no.1. A fragment of blade no.1 was found in the fuselage of the aircraft.
- ❑ The loss of the front of the engine no.1 was caused by a severe imbalance due to the loss of blade no.2 of the left propeller. The propeller went through the fuselage from one side to the other, without touching engine no.2. The imbalance was such that it caused the separation of the propeller and reduction gear assembly, upstream of the casing of the first compressor stage of the engine.

Separation of blade no.2 of the left propeller

- ❑ Blade no.2 separated from the propeller due to the fracture of the preload bolt, in the fillet radius, approximately 8.7 mm under the bolt head.
- ❑ The fracture of bolt no.2 was caused by crack propagation under fatigue loading, on 40% of its cross-section. The remaining 60% of cross-section broke in a brutal ductile manner, due to the overload.
 - A main crack and two secondary cracks were initiated on the side of the bolt.
 - Approximately 80 beach marks were counted between the initiation area of the main crack and the final fracture zone.
- ❑ The material of bolt no.2
 - had a hardness compliant with the specifications for steel grade S99
 - had a sulphur content that was slightly higher than the specifications for steel grade S99 (0.023w% +/- 0.003w% for a specified maximum of 0.020w%)
 - had a carbon content that was slightly higher than the specifications for steel grade S99 (0.45w% +/- 0.03w% for a specified maximum of 0.44w%)

Blade nos. 1, 3 and 4 of the left propeller

- ❑ no crack was detected in the fillet radius of the preload bolt
- ❑ The material of bolt no.1
 - had a hardness compliant with the specifications for steel grade S99
 - had a chemical composition compliant with the specifications for steel grade S99
- ❑ The material of bolt nos. 3 and 4
 - Had carbon and sulphur contents compliant with the specifications for steel grade S99

Other equipment of the left propeller

- ❑ the blade bearings of blade nos.1, 3 and 4 were properly lubricated, the greases used were in accordance with the manufacturer's specifications, anti-fretting paste (FRIN) was used.
- ❑ the blade bearing of blade no.2 was greased. It is not possible to say whether FRIN was used, because of the substantial presence of earth in the event bearing.
- ❑ The damage observed on the bearings was consecutive to the separation of blade no.2.
- ❑ The bearing preload, measured during disassembly, was below the values specified in OHM. However, these values were specified for assembly only. No value was specified for dismantling.

Other propellers examined

- ❑ The preload of certain bearings, measured during disassembly, was below the values specified in the OHM. Similarly, the values specified in the OHM were for assembly only.
- ❑ The bearings of the blade roots were properly lubricated, anti-fretting paste (FRIN) was used.

Maintenance

- ❑ The maintenance operations were up to date, according to the applicable schedule.
- ❑ The work cards for the last overhaul of the propeller were no longer available, the maintenance organization having ceased all maintenance activity on this type of propeller. This was consistent with the regulations in force on the date of the event.

APPENDICES**APPENDIX 1****Magnetic particle inspection of bolt nos. 1, 3 and 4 of the left propeller of I-MLVT****APPENDIX 2****Measurements of the rate per unit area of inclusions on the surface by image analysis**

APPENDIX 1

Magnetic particle inspection of bolt nos. 1, 3 and 4 of the left propeller of I-MLVT

Ce document de travail est la propriété du BEA et ne peut être communiqué ou reproduit même partiellement sans son autorisation écrite

Document Technique

Contrôle par magnétoscopie des vis de pied de pale

Identification du rapport : **BEA_i-vt131025_tec08**
 Date d'occurrence : 25/10/2013
 Lieu d'occurrence : AD Paris Charles de Gaulle (95)
 Type d'aéronef : FOKKER F 27 500
 Immatriculation : **I-MLVT**
 Equipements examinés :

Vis de fixation de pied de pale #1	Vis de fixation de pied de pale #3	Vis de fixation de pied de pale #4
Dowty-Propellers P/N : RA58592-1 S/N : EPK154	Dowty-Propellers P/N : RA58592-1 S/N : EPK155	Dowty-Propellers P/N : RA58592-1 S/N : EPK165

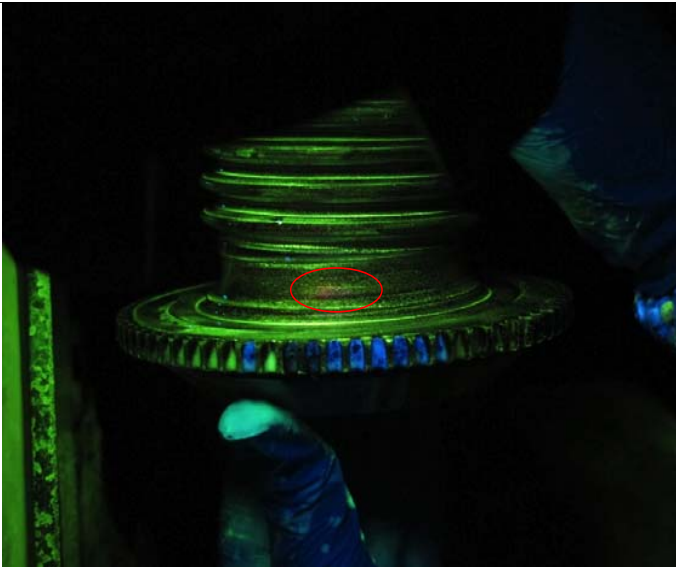
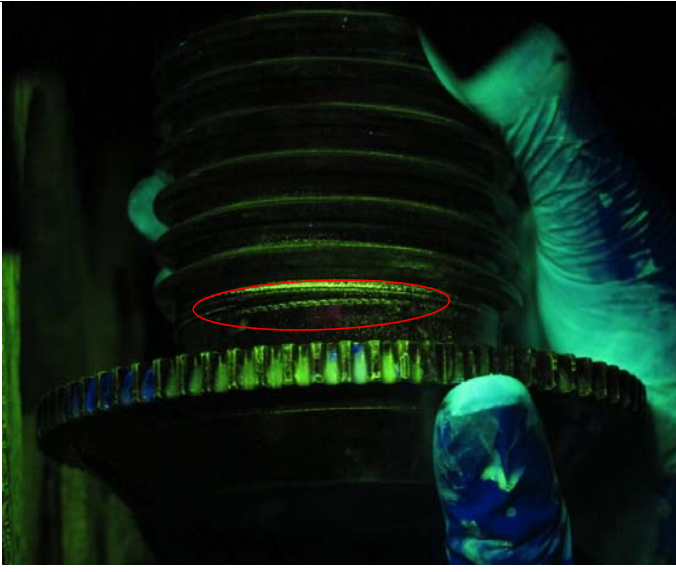
Travaux réalisés :

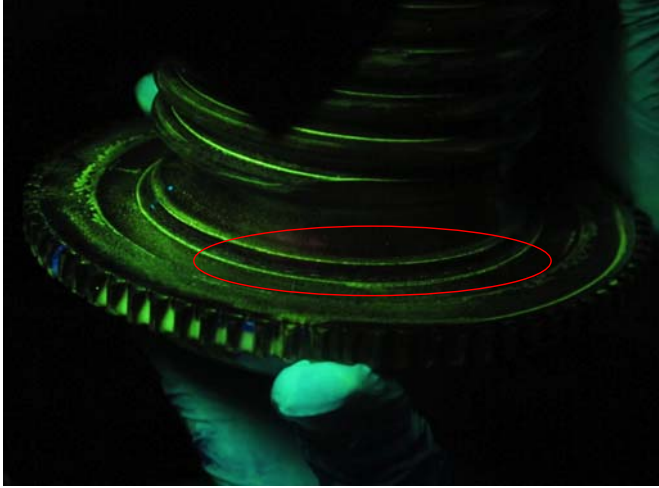
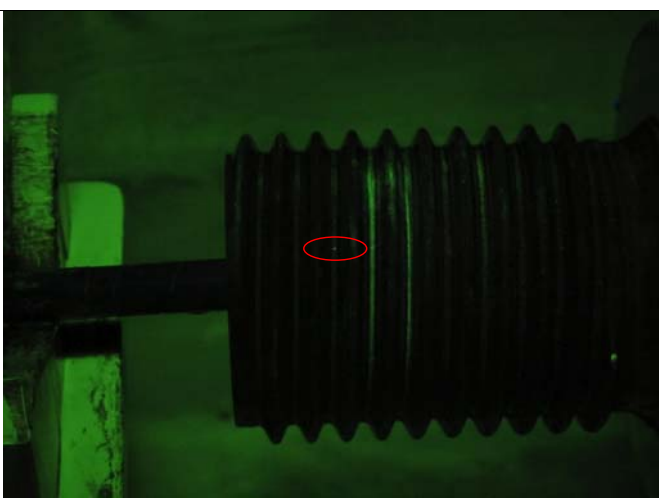
Le 18 décembre 2013, après le démontage de l'hélice gauche du Fokker 27 immatriculé I-MLVT à l'atelier de PropTech (Grande-Bretagne), un contrôle par magnétoscopie a été réalisé sur les vis de fixation des pales n°1, 3 et 4. Pour rappel, la vis de fixation de la pale n°2 a été retrouvée rompue à l'issue de l'événement.

Le contrôle a été réalisé par un opérateur agréé de PropTech, selon la procédure NDT26-M-SPM (document Dowty), tel que spécifié dans le manuel de maintenance de l'hélice. Deux enquêteurs du BEA y ont assisté.

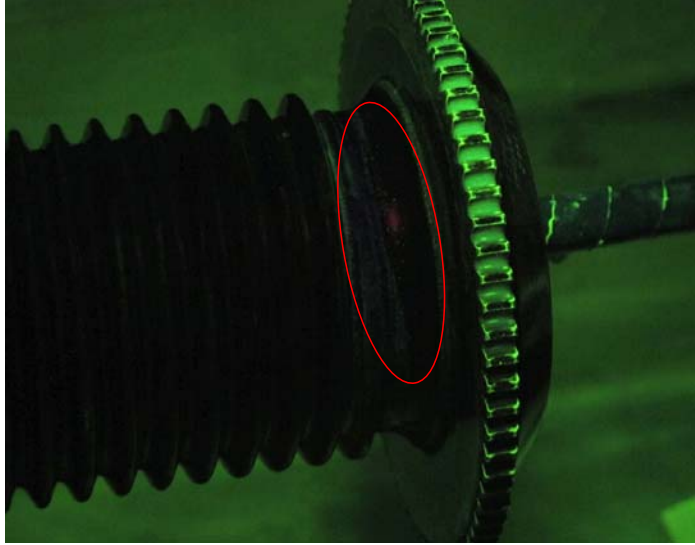
Ce document présente les indications observées au cours du contrôle de magnétoscopie. Des examens complémentaires doivent permettre de caractériser ces indications.

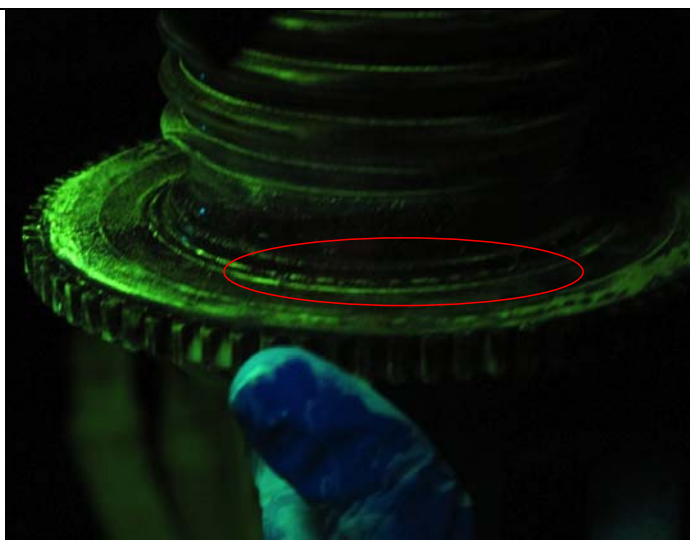
Résultats :

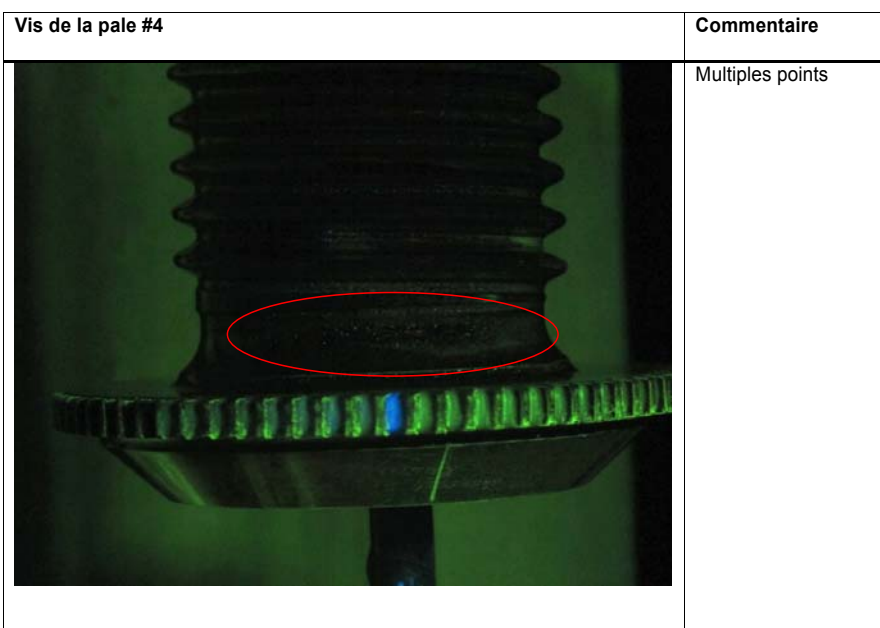
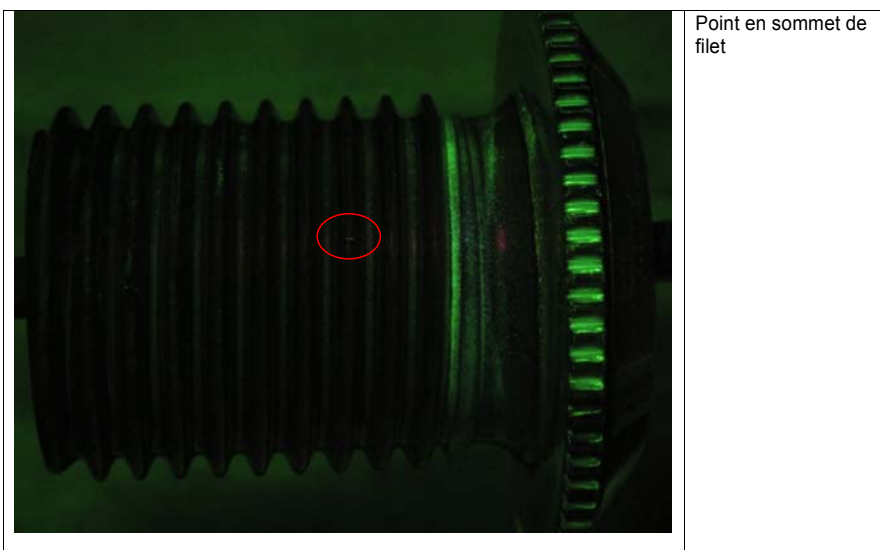
Vis de la pale #1	Commentaire
 A fluorescence image of a propeller blade. The blade is illuminated with a blue light, causing it to glow. A single, horizontal red line is visible on the blade's surface, circled in red. The background is dark.	ligne
 A fluorescence image of a propeller blade, similar to the one above. Three parallel, horizontal red lines are visible on the blade's surface, circled in red. The background is dark.	3 lignes discontinues parallèles

	1 ligne discontinue
	Point en fond de filet

	Point en fond de filet
-----------------------------------------------------------------------------------	------------------------

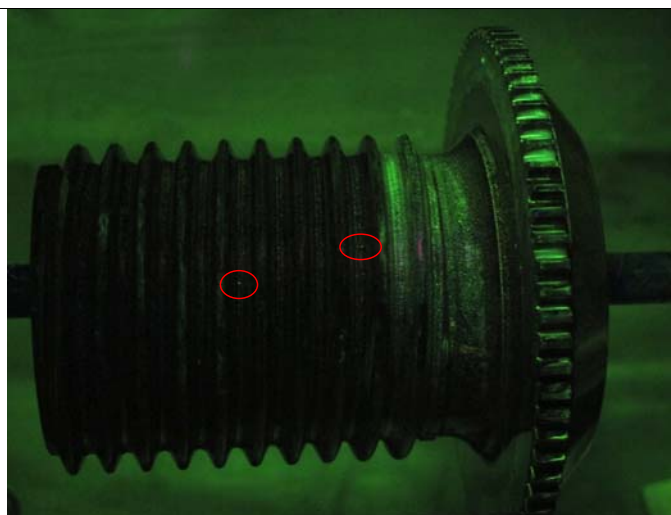
Vis de la pale #3	Commentaire
	Multiple points

	ligne
	Ligne discontinue





Multiples points +
quelques lignes



Points en fond de filet

APPENDIX 2

measurements of the rate per unit area of inclusions on the surface by image analysis

Measurements of the rate per unit area of inclusions on the surface were performed on a cross-section of bolt no.1, as well as on a cross-section of bolt no.2. On each section, 3 sets of 20 images were taken using an inverted microscope, at a magnification of x500, according to the areas shown in white in Figure 79.

The «core» area was taken at the core the bolt, in the longitudinal axis of the part. The «surface» area was taken near the outer surface of the bolt, still parallel to the longitudinal axis. The «surface-to-core» zone was an area from the surface to the core, according to an axis transverse to the diametrical plane, and selected in the plane of a thread root for bolt no.2 and the radius for bolt no.1.

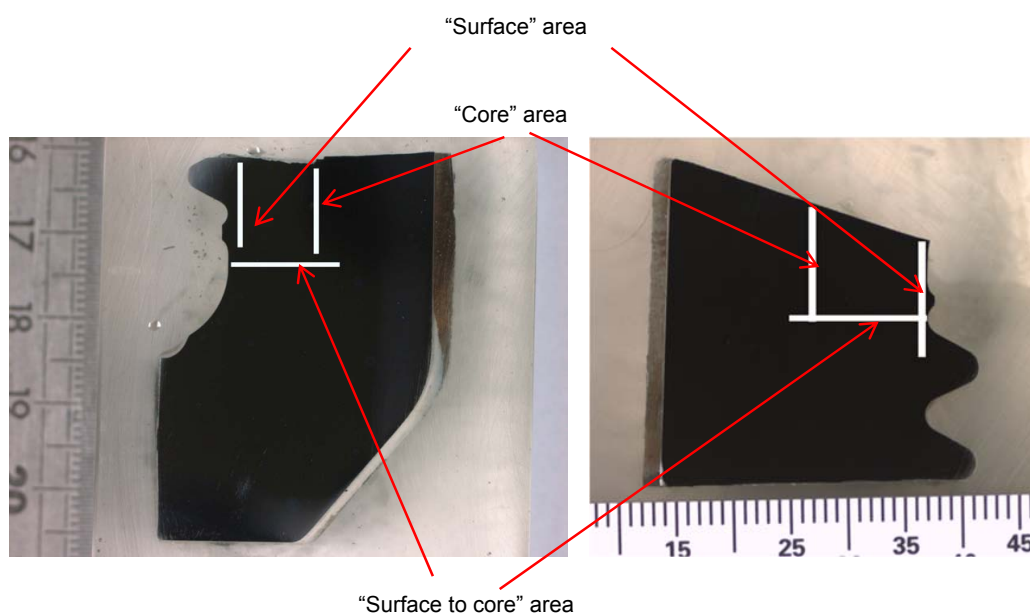


Figure 79: Cross-sections of bolt no.1 (left) and bolt no.2 (right) - the white areas were used to calculate the rate per unit area of inclusions on the surface

ImageJ software was used to process the images obtained in order to identify and isolate the inclusions and to calculate the rate per unit area of inclusions on the surface using the method described below and shown Figure 80 to Figure 83.

The raw image obtained by inverted microscopy was first of all converted to a grey level image. Then, the «adjust/threshold» option automatically provided a definition of the threshold grey level value, which revealed (in red in Figure 82) the darker areas of the picture, in this case the inclusions. The threshold could be adjusted manually by the user to include inclusions not taken into account automatically by the algorithm or to exclude image artefacts or related to the cross-section. On validating the threshold, the image was converted to black and white (binary image), in which the inclusions were shown in black. The surface inclusion rate on the resulting image was then obtained by dividing the number of black pixels by the total number of pixels.

The results were displayed in graph form, the value of the inclusion rate obtained on each image was displayed (discrete patterns) as well as the average obtained per zone (solid line), for each area («surface», «core» and «surface-to-core»).

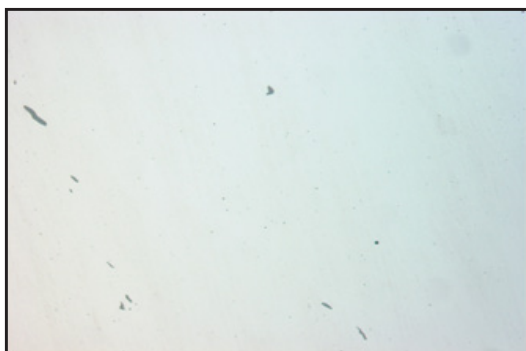


Figure 80: raw image taken by inverted microscope

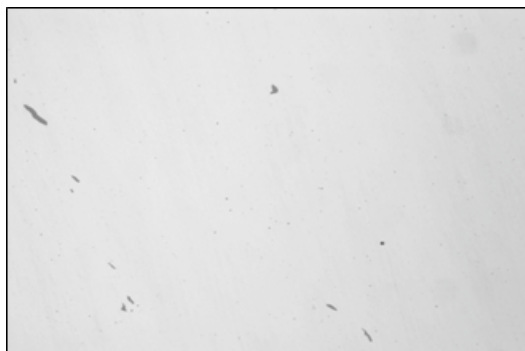


Figure 81: image converted to grey level



Figure 82: definition of the grey level threshold for identification of inclusions (in red)



Figure 83: binary image, the result of the processing process. The inclusions are shown in black

Bolt no.1:

For bolt no.1, the surface rate could be compared with the core rate (Figure 84). It could be seen that the cloud of points corresponding to each core and surface image merged, with an average value for the inclusion rate slightly lower on the surface (0.11% against 0.13% for the core). Locally, however, inclusions on the surface were found to be larger or more concentrated, the maximum rate being obtained on an image taken on the surface (0.34%).

When observing the evolution of the rate of inclusions from the surface to the core, obtained by analysis in the «surface-to-core» area, we found that whatever trend line chosen, it decreased, with a higher rate on the surface than at the core. This information remained local, valid only in the area under study (corresponding to imaging) of 0.49 mm wide and approximately 12 mm long, i.e. approximately 6 mm².

Finally, the maximum inclusion rate for this area is 0.74%. The corresponding image was shown in Figure 86 and had a particularly large inclusion, which explained the high area rate relative to other images.

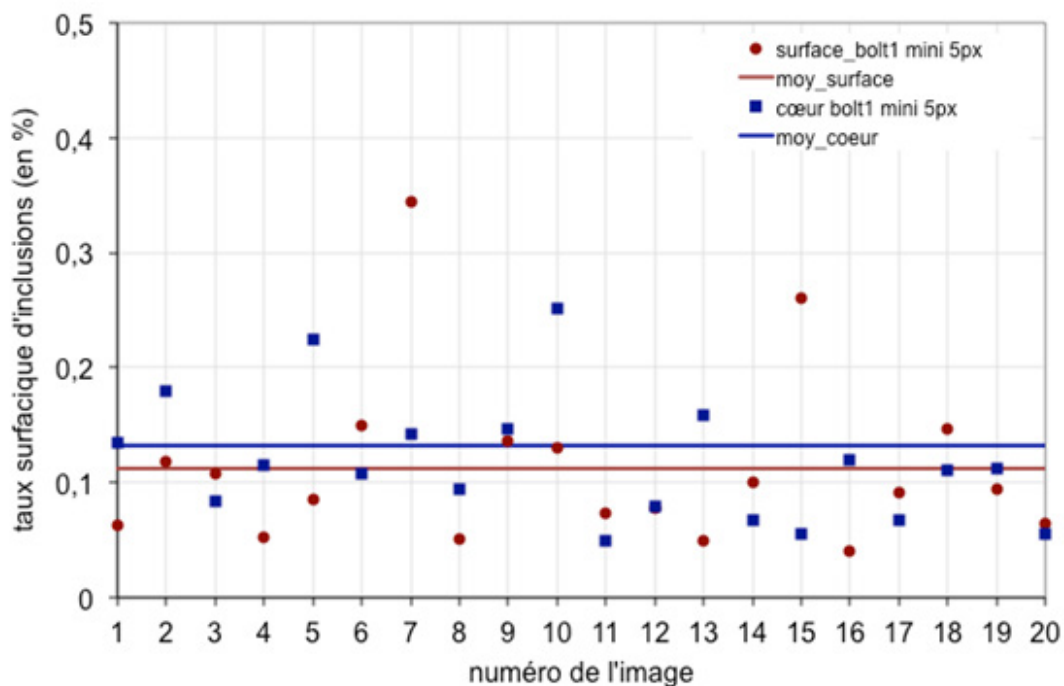


Figure 84: inclusion rate on the surface and core, bolt no.1.

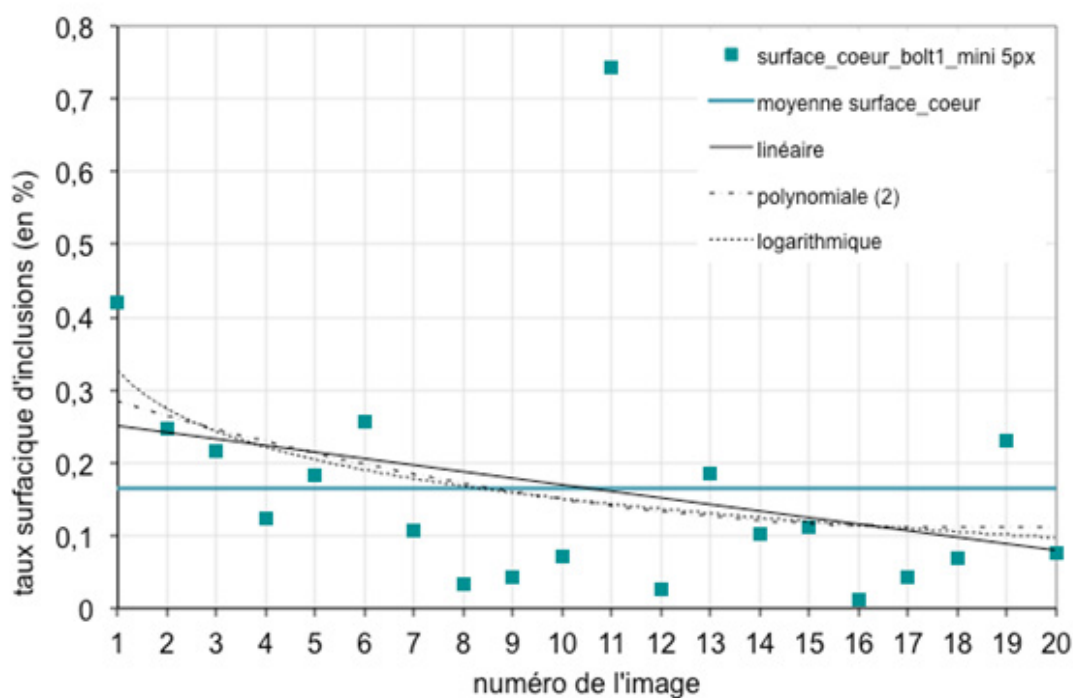


Figure 85: inclusion rate from the surface to the core (image 1: surface, image 20: core)

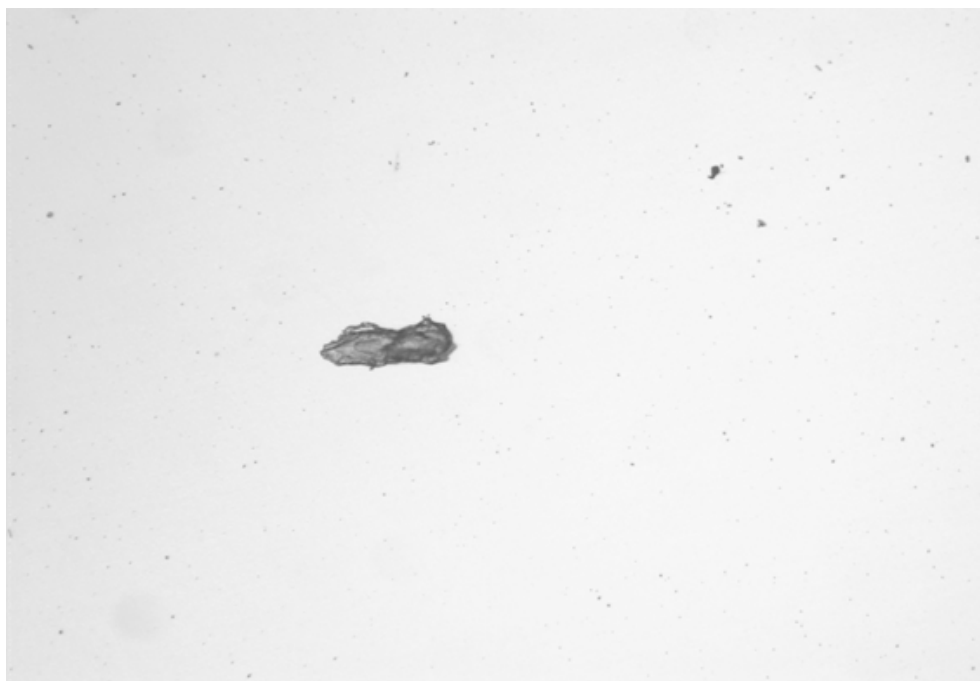


Figure 86: image 11, surface-to-core zone of bolt no.1
(image dimensions: 490 μm x 614 μm i.e. 0.3mm²)

Bolt no.2:

The same exercise was carried out on bolt no.2, the results are presented below. The inclusion rate was again on average higher at the core (0.13% against 0.10% on the surface), but the dispersion of the surface values was a little larger than previously. These mean values were similar to those for bolt no.1.

If we look at the evolution of the rate from the surface to the core («surface-to-core» zone, Figure 88), it can be seen that the average is less than 0.10%, that all of the values are below 0.20% and that the maximum value obtained is 0.61%. This value was obtained on Figure 89. It was easier to understand that the rate was high in this image, which was not representative of most of the images taken.

If this image was not taken into account, no change in the rate of inclusions was observed from the surface to the core.

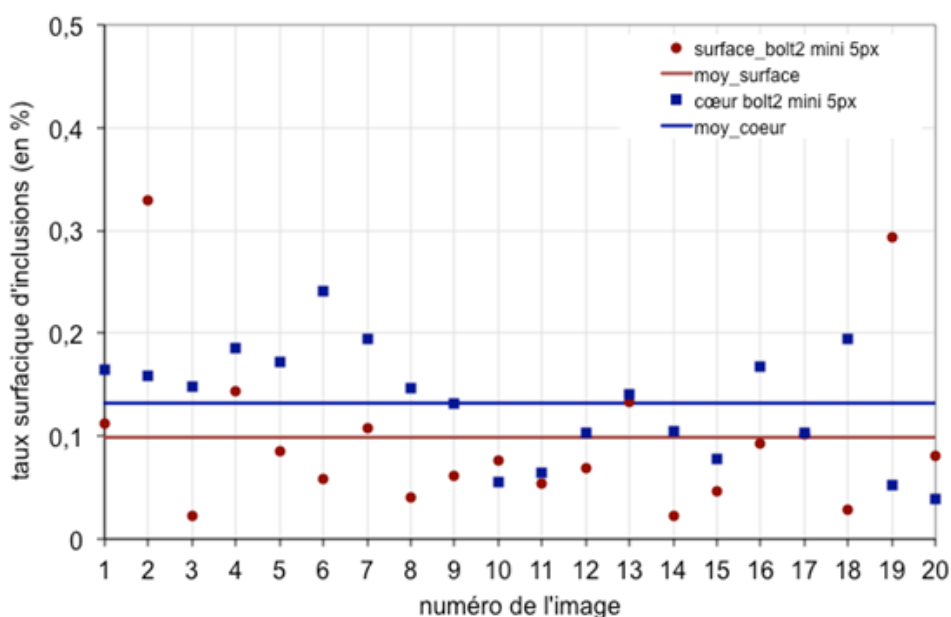


Figure 87: inclusion rate on the surface and core, bolt no.2.

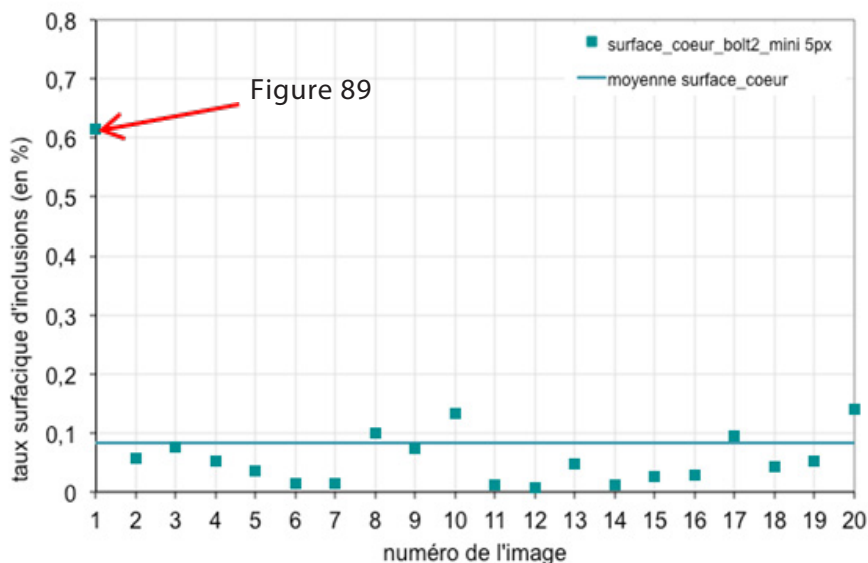


Figure 88: inclusion rate from the surface to the core
(image 1: surface, image 20: core)



Figure 89: age 1, surface-to-core zone of bolt no.2
(image dimensions: 490 μm x 614 μm i.e. 0.3mm²)

Conclusions

It is not possible to tell on the basis of these measurements by image analysis whether bolt no.2 had more inclusions than bolt no.1. On the contrary, the average rates for sulphides measured on bolts nos.1 and 2 were rather similar. The inclusion rate may have been locally high, both on bolt no.1 and on bolt no.2. In addition, it was not possible to determine whether more inclusions were present on the surface of the part relative to the core, either on bolt no.1 or on bolt no.2. Even if the trend observed in Figure 85 in the «surface-to-core» area of bolt no.1 decreased from the surface to the core, this information remained local and the inclusion rate is on average higher at the core than on the surface on the areas of this bolt that were studied.

Since this study was limited to a few areas, the existence of a local concentration of inclusions could not be excluded.



BEA

Bureau d'Enquêtes et d'Analyses
pour la sécurité de l'aviation civile

10 rue de Paris
Zone Sud - Bâtiment 153
Aéroport du Bourget
93352 Le Bourget Cedex - France
T : +33 1 49 92 72 00 - F : +33 1 49 92 72 03

www.bea.aero

